Acta Protozool. (2008) 47: 1–33

ACTA
PROTOZOOLOGICA

Morphology, Ontogenesis and Molecular Phylogeny of *Neokeronopsis* (*Afrokeronopsis*) *aurea* nov. subgen., nov. spec. (Ciliophora: Hypotricha), a New African Flagship Ciliate Confirms the CEUU Hypothesis

Wilhelm FOISSNER[1] and Thorsten STOECK[2]

[1]Universität Salzburg, FB Organismische Biologie, Salzburg, Austria; [2]Universität Kaiserslautern, FB Biologie, Kaiserslautern, Germany

Summary. *Neokeronopsis* (*Afrokeronopsis*) *aurea* nov. subgen., nov. spec. was discovered in soil from the floodplain of a small river in the Krueger National Park, Republic of South Africa. Its morphology, ontogenesis, and 18S rDNA were studied with standard methods. Furthermore, we supplemented the data on *N.* (*N.*) *spectabilis* by reinvestigating the preparations deposited in the British Museum of Natural History. *Neokeronopsis* (*Afrokeronopsis*) *aurea* is a very conspicuous ciliate because it has an average size of 330 × 120 µm and is golden yellow due to the orange-coloured cytoplasm and citrine cortical granules. Further main characteristics include the semirigid body; the urostylid cirral pattern with a distinct corona of frontal and pseudobuccal cirri both originating from the midventral rows; multiple anterior fragmentation of dorsal kineties 1–3; multiple posterior fragmentation of kinety 3, commencing with an unique whirl of kinetofragments; three caudal cirri; an oxytrichid/cyrtohymenid oral apparatus with polystichad paroral membrane and buccal depression; a single oral primordium developing along the transverse cirral row; and an oxytrichid 18S rDNA. These peculiarities are used to establish the new oxytrichid family Neokeronopsidae, the new subgenus *Afrokeronopsis*, and the new species *N.* (*A.*) *aurea*. Further, these features confirm the CEUU hypothesis, i.e., convergent evolution of a midventral cirral pattern in urostylid and oxytrichid hypotrichs; additionally, *N.* (*A.*) *aurea* is the first (semi)rigid hypotrich with cortical granules and the second one with midventral rows, breaking the granule and flexibility dogmas. These and other observations show that the phylogeny of the hypotrichs is full of convergences. Thus, only a combined effort of classical and molecular phylogeneticists will provide the data needed for a natural classification. Based on the CEUU hypothesis, the molecular data, and literature evidence, we suggest that midventral oxytrichids should be ranked as distinct families; accordingly, we establish a further new family, the Uroleptidae, which forms a distinct clade within the oxytrichid molecular trees. *Neokeronopsis* is possibly related to *Pattersoniella* because it has the same special mode of forming the buccal cirri and possesses a buccal depression found also in *Steinia*, a close relative of *Pattersoniella*. The large size and conspicuous colour make *N.* (*A.*) *aurea* a biogeographic flagship possibly confined to Africa or Gondwana, while *Neokeronopsis* (*N.*) *spectabilis* (Kahl, 1932) is an Eurasian flagship.

Key words: Biogeography, buccal depression, floodplain soil, Krueger National Park, Neokeronopsidae nov. fam., *Pattersoniella*, pseudobuccal cirri, *Steinia*, Stichotrichida, Uroleptidae nov. fam.

INTRODUCTION

Hypotrichs have fascinated already the ancient protistologists, such as Ehrenberg (1838), Stein (1859),

Address for correspondence: Wilhelm Foissner, Universität Salzburg, FB Organismische Biologie, Hellbrunnerstrasse 34, A-5020 Salzburg, Austria; E-mail: Wilhelm.Foissner@sbg.ac.at

Bütschli (1889), and Wallengren (1900), because the distinctness of the cirri makes it possible to recognize species-specific patterns and to follow pattern ontogenesis without complicated staining procedures. Indeed, hypotrichs were among the first ciliates for which reliable investigations on ontogenesis have been reported (Stein 1859, Wallengren 1900). When silver methods revolutionized ciliate research, the hypotrichs were again among the first for which detailed data became available because they were more easily to impregnate than many other ciliates (Tuffrau 1960, Tuffrau *et al*. 1968).

Recently, Berger (1999, 2006) monographed part of the hypotrichs, showing the great knowledge that accumulated on their morphology, ontogenesis, and biology. Furthermore, molecular data became available for most main groups (~ families) and some species complexes (Berger 2006, Schmidt *et al*. 2007). In spite of this, evolution and classification of the hypotrichs remained highly controversial, both at morphologic and molecular level (for reviews, see Berger 1999, 2006; Foissner *et al*. 2004, Schmidt *et al*. 2007). One of the most disappointing discrepancies between classical and molecular phylogenies concerned the occurrence of typical midventral hypotrichs (urostylids with two rows of zigzagging cirri in midline, e.g., *Urostyla grandis*) among the oxytrichids, a large assemblage of species with a highly characteristic pattern usually consisting of 18 fronto-ventral-transverse cirri (18 FVT cirral pattern, e.g., in *Stylonychia mytilus*).

This fundamental disagreement in morphologic and molecular phylogenies stimulated the CEUU hypothesis (**C**onvergent **E**volution of **U**rostylids and **U**roleptids) which proposed that the urostylid midventral pattern evolved from an oxytrichine ancestor, developing a second time within the Oxytrichidae (Foissner *et al*. 2004). Foissner *et al*. (2004) could not provide a definite morphologic proof for the CEUU hypothesis because this would have required a hypotrich having the following attributes: a midventral cirral pattern; dorsomarginal kineties; fragmentizing dorsal kineties, preferable posterior fragmentation of kinety 3; and an oxytrichid small subunit (18S) ribosomal RNA sequence. Fortunately, such ciliate has been discovered now, viz., *Neokeronopsis* (*Afrokeronopsis*) *aurea*, which will be described in great detail in the present paper.

Our study shows the validity of the CEUU hypothesis, i.e., that even "very strong" morphologic features evolved convergently. Indeed, evolution of the hypotrichs appears full of homoplasies. For instance, a recent molecular study suggests that even the 18 FVT cirral pattern, which is considered a very stable evolutionary feature (Berger 1999), evolved several times (Schmidt *et al*. 2007). The same applies to another "strong" morphologic character, viz., body flexibility/rigidity which is not as stable as it has been assumed (Berger 1999, Foissner and Stoeck 2006).

The hypotrichs with their high variety of cirral and ontogenetic patterns could play a major role in understanding evolution and classification of ciliates, especially below the ordinal rank. However, testable evolutionary hypotheses are rare, possibly because researchers underestimated the extent of homoplasy and diversity, thus becoming unable to abstract hypotheses from the data available. Taking into account these problems, we shall propose some hypotheses and translate them into classification units. Presently, about 600 valid hypotrich species have been described (H. Berger, pers. inform.). However, this is only the tip of the iceberg because new taxa are described at a high rate (Berger 2006), and the senior author has about 250 undescribed hypotrichs, mainly from soils globally, in his notes. These many new taxa will make "small" genera and families larger and more reliable.

MATERIALS, METHODS AND TERMINOLOGY

Materials

Neokeronopsis (*Afrokeronopsis*) *aurea* was discovered in the Republic of South Africa, i.e., in a soil sample from the bank (active floodplain) of the Matjula River in the surroundings of the Berg-en-dal Lodge, E31°28′ S25°20′. The Matjula River is a small tributary to the large Crocodile River at the southern border of the Krueger National Park. The wet soil was collected from the upper 0–10 cm together with some plant litter and grass roots. The sample was taken in February 1995, air-dried for one month, and stored in a plastic bag.

A second population of *N.* (*A.*) *aurea* was discovered in soil (pH 6.5) from the dry bed of the Mlambane River, about 10 km north of the Berg-en-dal Lodge. This population, which is highly similar to the type, will be described later. Here, we use it mainly for discussion of biogeographic aspects.

Further, we studied the protargol slides of *N.* (*N.*) *spectabilis* deposited by Warren *et al*. (2002) in the British Museum of Natural History.

Cultivation

In 2006, that is, 11 years after collection, the sample was rewetted with distilled water to obtain a non-flooded Petri dish culture, as described in Foissner *et al*. (2002). To increase organismal activity and filter capacity of the very fine-grained, alluvial soil, we added some sterilized, chopped wheat straw. This sample yielded an extraordinarily diverse ciliate community with about 150 species, of which at least 30 were undescribed. *Neokeronopsis* (*A.*) *aurea* was

sparse. Thus, we isolated some specimens to set up cultures in Eau de Volvic (French mineral water) enriched with some squashed wheat grains to stimulate growth of bacteria and flagellates (*Polytomella*, *Rhodomonas*). Further, the ciliate *Colpidium kleini* was added as a food source, but was rarely ingested. Most specimens fed on starch grains from the squashed wheat kernels and/or on flagellates.

Morphological methods

Living cells were studied using a high-power oil immersion objective and interference contrast. Protargol impregnation and scanning electron microscopy (SEM) were performed as described by Foissner (1991). However, *Neokeronopsis* (*A.*) *aurea* was extremely difficult to preserve. Thus, for protargol impregnation we added 1 ml of 2% aqueous osmium tetroxide to each 10 ml of Stieve's fluid and fixed cultures in toto because cells usually burst when added dropwise. All manipulations on fixed cells were done with fine pipettes because cells tended to break when centrifuged. In spite of much effort, good SEM preparations were not obtained.

Counts and measurements on silvered specimens were performed at a magnification of × 1.000. *In vivo* measurements were conducted at magnifications of × 40–1.000. Drawings of live specimens were based on free-hand sketches and micrographs; those of impregnated cells were made with a drawing device. In the ontogenetic stages, parental structures are shown by contour, while newly formed structures are shaded black.

Molecular methods

For analysis of the 18S rDNA sequence, 30 specimens were isolated with a micropipette from a pure culture, washed in Eau de Volvic, and transferred into 180 µl ATL buffer (Qiagen) and 20 µl Proteinase K (20 mg/ml). Subsequently, the genomic DNA was extracted using the protocol for cultivated animal cells of the DNEasy Tissue Kit (Qiagen), according to the manufacturer's instructions. We used standard isopropanol precipitation to concentrate the extracted nucleic acids. Amplification of the 18S rDNA fragment was performed via PCR using the universal eukaryotic primers EukA and EukB (Medlin *et al*. 1988), while cloning was performed as described by Stoeck and Epstein (2003). Three positively screened (M13 reamplification) plasmids were sequenced bidirectionally with MWG (Ebersheim, Germany).

We aligned the 18S rDNA sequence to available Oxytrichinae, Stylonychinae and Urostylidae sequences using Clustal X (Thompson *et al*. 1997). The alignments were manually refined in MacClade (Maddison and Maddison 2003), according to conserved regions. We applied the program Modeltest (Posada and Crandall 1998) to choose the model of DNA substitution that best fits our data sets from among 56 possible models. Maximum parsimony, evolutionary distance, and maximum likelihood trees we calculated using the PAUP software package 4.0b10 PAUP (Swofford 2002), while a Bayesian inference tree was obtained by using Mr. Bayes (Ronquist and Huelsenbeck 2003). The DNA substitution model as well as parameter settings for the trees constructed are described in the legend to Figure 38. We assessed the relative stability of tree topologies using 1,000 bootstrap replicates and posterior probabilities of 751 Bayesian trees. Heuristic searches for bootstrap analyses employed stepwise addition, starting trees with simple addition of sequences and TBR branch-swapping. Bootstrap analyses settings were chosen according to the Modeltest output. For the Bayesian tree we ran two simultaneous, completely independent analyses starting from different random trees. The analysis also employed GTR+I+G as the DNA substitution model with the gamma distribution shape parameter, the proportion of invariable sites, base frequencies, and a rate matrix for the substitution model as assessed by Mr. Bayes. Metropolis coupling with 3 heated chains and one "cold" chain was employed to improve the Markov Chain Monte Carlo sampling of the target distribution. We ran 1,000,000 generations and sampled every 1,000th generation, resulting in 1,001 samples from the posterior probability distribution. Then, rooted and unrooted trees were calculated. All methods resulted in congruent trees (Fig. 38), that is, none assigned *N.* (*A.*) *aurea* to the Urostyloidea, as suggested by the midventral rows. All alignments and trees are available from the authors upon request.

Terminology

Terminology is according to Corliss (1979) and Foissner and Al-Rasheid (2006). The term "midventral rows" is used as defined by Berger (2006), that is, it designates a longitudinal series of zigzaging cirri in two rows near the ventral midline. A new term is the "buccal depression", i.e., a special concavity on the dorsal wall (bottom) of the buccal cavity. As yet, this structure has been found in only two genera, viz., *Steinia* (Kahl 1932, Voss and Foissner 1996) and *Neokeronopsis* (*Afrokeronopsis*) *aurea*. Further, we introduce the term "semirigid" as a category of body flexibility. This term applies to species which cannot be classified unambiguously in the rigid (e.g. *Stylonychia*) or flexible (e.g. *Oxytricha*) group. A further new term, pseudobuccal cirri, is explained in the section on "The origin of buccal cirri." Finally, the vernacular term "midventral oxytrichids" is introduced to designate that taxa which have urostylid-like midventral rows but appear within the oxytrichids in molecular trees, for instance, *Uroleptus* and *Neokeronopsis*.

Nomenclature follows the recent revision of Berger (2006), who maintains the time-honoured naming of Stein and Ehrenberg, and thus abandons the more recent stichotrichs. Accordingly, Berger (2006) distinguishes the Hypotricha Stein, 1859 (e.g. *Oxytricha*, *Urostyla*; now widely named Stichotrichida) and the Euplota Ehrenberg, 1830 (e.g. *Euplotes*, *Uronychia*; now widely named Hypotrichida).

RESULTS

Uroleptidae nov. fam.

Diagnosis: Very flexible midventral hypotrichs forming a distinct clade within the oxytrichids in molecular trees.

Type genus: *Uroleptus* Ehrenberg, 1831.

Remarks: See "CEUU hypothesis and molecular trees" in the Discussion section for a detailed justification of this new family.

Neokeronopsidae nov. fam.

Diagnosis: Rigid or flexible, oxytrichid Hypotricha with midventral (urostylid) cirral pattern, including a more or less distinct corona of frontal and pseudobuccal

cirri both originating from the midventral rows. Oral apparatus in *Oxytricha* or mixed *Oxytricha*/*Cyrtohymena* pattern. Dorsal ciliature composed of dorsomarginal kineties and three ordinary rows producing further kineties by multiple fragmentation; parental dorsal ciliature resorbed or partially conserved after ontogenesis.

Type genus: *Neokeronopsis* Warren, Fyda and Song, 2002.

Taxa assignable: *Neokeronopsis* Warren *et al*., 2002; *Neokeronopsis* (*Afrokeronopsis*) nov. subgen; *Pattersoniella* Foissner, 1987.

Nomenclature: We include in the new family the genus *Pattersoniella*, for which Foissner (1987) established the family Pattersoniellidae, according to Shi *et al*. (1999). However, Foissner (1987) did not create such family, neither in the paper referred to by Shi *et al*. (1999) nor in any other study, but classified *Pattersoniella* in the Oxytrichidae (Berger 1999, 2006).

We shall never know whether Shi *et al*. (1999) made a mistake or intended to establish a new family Pattersoniellidae. Thus, this family is suspect nomenclaturally, suggesting a correct, new start, that is, to establish a new family Neokeronopsidae including *Pattersoniella* as a second genus.

Neokeronopsis Warren, Fyda and Song, 2002

Improved diagnosis: Very flexible or semirigid Neokeronopsidae with conspicuous midventral rows and frontal cirral corona, each composed of many cirri, producing an urostylid cirral pattern. With many or only three caudal cirri. Oral apparatus in mixed *Oxytricha*/*Cyrtohymena* pattern and without or with buccal depression. Oral primordium developing postorally and mainly above transverse cirral row or mainly along the latter; multiple fragmentation of dorsal kinety 3 produces a conspicuous whirl of kinetofragments. Parental dorsal ciliature resorbed.

Type species: *Neokeronopsis spectabilis* (Kahl, 1932) Warren *et al*., 2002. Basionym: *Holosticha* (*Keronopsis*) *spectabilis* Kahl, 1932.

Remarks: We split the genus into two subgenera. See Warren *et al*. (2002), Berger (2006), and Wang *et al*. (2007) for redescriptions of the type species, neotypification problems, and etymology.

Neokeronopsis (*Neokeronopsis*) nov. stat.

Diagnosis: Very flexible Neokeronopsidae with smooth dorsal buccal wall and many caudal cirri; oral primordium developing postorally and above transverse cirral row.

Type species: *Neokeronopsis* (*Neokeronopsis*) *spectabilis* (Kahl, 1932) Warren *et al*., 2002. Basionym: *Holosticha* (*Keronopsis*) *spectabilis* Kahl, 1932.

Neokeronopsis (*Afrokeronopsis*) nov. subgen.

Diagnosis: Semirigid Neokeronopsidae with buccal depression and three caudal cirri; oral primordium developing along transverse cirral row.

Type species: *Neokeronopsis* (*Afrokeronopsis*) *aurea* nov. spec.

Etymology: Composite of the Latin noun *Africa* and the Greek generic name *Keronopsis*, as explained in Berger (2006).

Pattersoniella Foissner, 1987

Improved diagnosis: Rigid Neokeronopsidae with inconspicuous midventral rows and frontal cirral corona, each consisting of comparatively few cirri, producing a mixed oxytrichid/urostylid cirral pattern. Three caudal cirri. Oral apparatus oxytrichid, without buccal depression. Oral primordium developing very near to two postoral midventral cirri and mainly above transverse cirral row. Parental dorsal ciliature partially maintained.

Type species: *Pattersoniella vitiphila* Foissner, 1987.

Remarks: In diagnosing this genus, its similarity with *Neokeronopsis* becomes apparent, i.e., the differences are quantitative, except for the conservation of some parental dorsal ciliature, a rare feature. However, the rather distinct genetic divergence suggests not only maintenance of both genera (Fig. 38), but also indicates convergent evolution of some features (for details, see Discussion). We checked the type population for fragmentation of dorsal kineties 1 and 2; definitely, any fragmentation is lacking.

Description of *Neokeronopsis* (*Afrokeronopsis*) *aurea* nov. spec.

Diagnosis: Size about 330 × 120 µm *in vivo*; obovate; with golden sheen under oblique illumination due to the orange-coloured cytoplasm and numerous citrine cortical granules forming narrow strands ventrally and dorsally. Two ellipsoidal macronucleus nodules. Midventral rows distinctly apart, composed of an average of 19 pairs of cirri. Frontal corona consisting of 13 cirri on average; buccal row composed of 12 cirri, hook-shaped with main portion close to right margin of buccal cavity. On average 24 transverse cirri forming a long, J-shaped row commencing underneath buc-

Table 1. Morphometric data on *Neokeronopsis* (*Afrokeronopsis*) *aurea* sp. n.

Characteristics[a]	$\bar{x}$	M	SD	SE	CV	Min	Max	n
Body, length	306.4	303.0	25.9	5.7	8.5	260.0	350.0	21
Body, width	111.8	110.0	12.9	2.8	11.5	86.0	135.0	21
Body length:width, ratio	2.8	2.8	0.3	0.1	9.1	2.2	3.4	21
Anterior body end to left end of adoral zone, distance	117.5	117.0	5.3	1.2	4.5	108.0	130.0	21
Percentage (%) of body length occupied by AZM	38.6	38.7	2.7	0.6	7.0	34.1	45.2	21
Anterior body end to right end of adoral zone, distance	82.9	82.0	6.3	1.4	7.6	73.0	100.0	21
Right and left end of adoral zone, distance in main body axis	35.1	35.0	4.8	1.1	13.8	26.0	42.0	21
Longest adoral membranelle, length	17.4	17.0	1.2	0.3	6.7	16.0	20.0	21
Buccal field, maximum width	25.1	26.0	2.9	0.6	11.3	20.0	30.0	21
Anterior body end to right marginal row, distance	89.8	88.0	8.5	1.9	9.5	74.0	105.0	21
Anterior body end to frontoterminal cirri, distance	89.4	88.0	9.5	2.1	10.6	75.0	115.0	21
Anterior body end to first midventral pair, distance[b]	91.5	91.0	8.2	1.8	9.0	72.0	107.0	21
Anterior body end to anteriormost transverse cirrus, distance	126.7	123.0	9.1	2.0	7.2	115.0	147.0	21
Midventral rows in mid-body, distance in between	6.6	7.0	0.8	0.2	12.2	5.0	8.0	21
Posterior body end to right marginal row, distance	7.5	7.0	2.9	0.6	38.9	2.0	13.0	21
Posterior body end to posteriormost transverse cirrus, distance	14.5	14.0	2.2	0.5	14.9	11.0	19.0	21
Anterior body end to begin of paroral, distance	32.1	32.0	2.1	0.5	6.6	28.0	36.0	21
Anterior body end to proximal end of paroral, distance	104.1	103.0	6.0	1.3	5.7	92.0	117.0	21
Anterior body end to begin of endoral, distance	42.1	42.0	2.3	0.5	5.5	38.0	46.0	21
Anterior body end to proximal end of endoral, distance	114.5	115.0	5.6	1.2	4.9	102.0	125.0	21
Anterior body end to first macronucleus nodule, distance	80.3	79.0	9.3	2.0	11.6	70.0	100.0	21
Macronucleus nodules, distance in between	45.9	43.0	9.4	2.1	20.5	34.0	65.0	21
Anterior macronucleus nodule, length	34.9	35.0	4.1	0.9	11.6	30.0	44.0	21
Anterior macronucleus nodule, width	20.4	21.0	3.4	0.8	16.8	13.0	25.0	21
Posterior macronucleus nodule, length	41.5	40.0	4.7	1.0	11.3	33.0	50.0	21
Posterior macronucleus nodule, width	17.4	18.0	3.0	0.7	17.2	8.0	22.0	21
Adoral membranelles, number	100.3	100.0	2.6	0.6	2.6	95.0	104.0	21
Macronucleus nodules, number	2.0	2.0	0.0	0.0	0.0	2.0	2.0	40
Frontal (coronar) cirri, number	12.8	13.0	1.0	0.2	8.2	11.0	14.0	21
Buccal cirri, number[b]	11.6	12.0	0.9	0.2	7.5	10.0	13.0	21
Frontoterminal cirri, number	2.0	2.0	0.0	0.0	0.0	2.0	2.0	21
Midventralcirri, number[b]	37.9	37.0	3.6	0.8	9.6	31.0	44.0	21
Transverse cirri, number	23.9	24.0	1.6	0.4	6.9	22.0	27.0	21
Right marginal cirri, number	50.4	52.0	4.7	1.0	9.3	43.0	57.0	21
Left marginal cirri, number	58.2	59.0	4.1	0.9	7.1	49.0	64.0	21
Caudal cirri, number[c]	3.0	3.0	0.0	0.0	0.0	3.0	3.0	38
Dorsal kineties, number[d]	14.1	14.0	1.4	0.3	9.6	12.0	17.0	21
Bristles in dorsal kinety 1, number	88.3	89.0	7.6	1.7	8.6	76.0	110.0	21
Bristles in dorsal kinety 2, number	62.7	63.0	6.1	1.3	9.7	48.0	74.0	21

[a] Data based on mercury chloride-osmium fixed, well preserved, morphostatic specimens from three different, exponentially growing cultures. All measurements in µm. AZM – adoral zone of membranelles, CV – coefficient of variation in %, M – median, Max – maximum, Min – minimum, n – number of specimens investigated, SD – standard deviation, SE – standard error of arithmetic mean, $\bar{x}$ – arithmetic mean.

[b] See description and Figure 14. Briefly, the number of cirri should be the same in the frontal corona and the buccal row because both originate from midventral pairs. However, the frontal corona has one additional cirrus due to the first frontal cirrus, which is produced by the undulating membranes.

[c] Among 40 specimens investigated, 1 had two caudal cirri and 1 had four.

[d] One to three, more or less scattered kinetids between rows or between first dorsomarginal row and right marginal cirral row not considered; likewise, the anterior fragments of kineties 1–3 were not counted.

cal vertex. Adoral zone impressive because occupying about 40% of body length, composed of an average of 100 membranelles, and extending far posteriorly (27%) along right body margin. Resting cysts 116 µm across on average, consist of an outer, about 25 µm thick, hyaline layer with polygonally facetted surface and an about 2 µm thick, compact inner layer.

Type locality: Floodplain soil from the Matjula River, i.e., from the surroundings of the Berg-en-dal Lodge near the southern border of the Krueger National Park, Republic of South Africa, E31°28′ S25°20′.

Type material: 2 holotype (ventral and dorsal view) and 8 paratype slides with protargol-impregnated morphostatic and dividing specimens from a pure culture

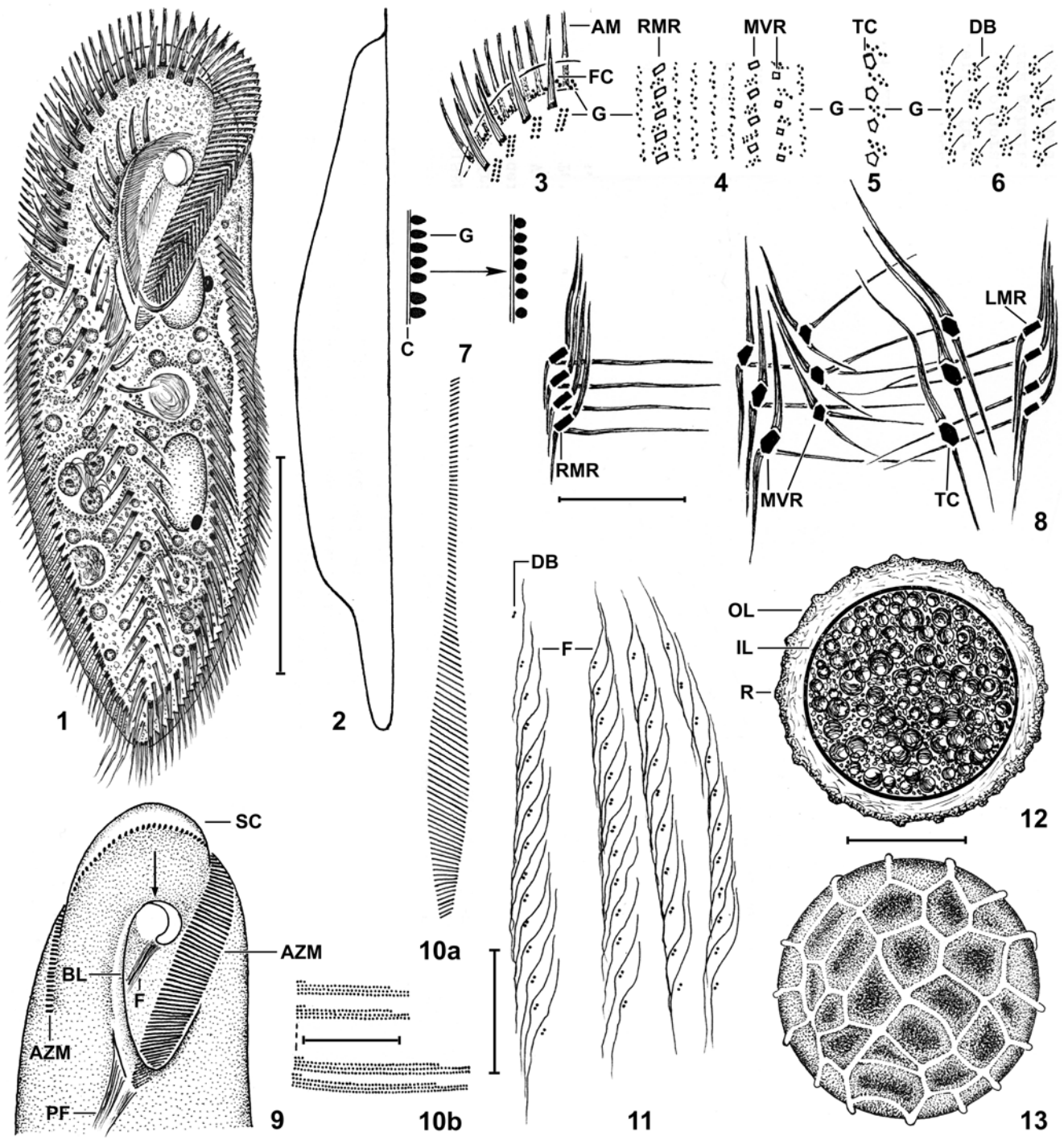

have been deposited in the Biology Centre of the Museum of Upper Austria, Linz (LI). The specimens shown in Figures 8, 10, 11, 14–17, 19, 20, 25–27, 39–61 and some other well-impregnated cells are marked by black ink circles on the coverslip. The 18S rDNA sequence of *N.* (*A.*) *aurea* has been deposited in GenBank (accession number EU124669). Two holotype specimens are necessary because the dorsal ciliature, which is a main species feature, cannot be seen clearly in the ventrally oriented specimen.

Etymology: The Latin adjective *aurea* (golden coloured) refers to the golden sheen the cells show under oblique illumination in the dissecting microscope.

Description (Figs 1–38): Size 280–380 × 90–140 µm, usually about 330 × 120 µm *in vivo*, decreases after prolonged cultivation, but cirral number changes hardly; length: width ratio near 2.8 both *in vivo* and protargol preparations (Table 1). Body shape obovate (2.2:1) to elongate obovate (3.4:1), sometimes slightly sigmoidal, widest in mid-body, posterior end narrowly rounded to bluntly pointed (Figs 1, 14, 15, 18–20, 38b, 61); dorsoventrally flattened 2–3:1, ventral side flat, dorsal convex with rear region sharply set off from flat posterior end (Fig. 2). Body semirigid as in *Sterkiella*, i.e., not as stiff as in *Stylonychia mytilus* and not as flexible as in *Oxytricha*; basically, however, (semi)rigid, as also indicated by the elaborate system of thick fibres associated with cirri and dorsal bristles (Fig. 8); slightly flexible and contractile (~ 10%) when touching obstacles and crawling on accumulations of organic mud, stiff like a board when swimming; becomes flexible under suboptimal conditions, both in pure culture and the non-flooded Petri dish culture. Difficult to preserve with ordinary fixatives (see Material and Methods section), but not sensitive to coverslip pressure. Nuclear apparatus in middle quarters of cell slightly left of body's midline (Figs 1, 14, 15, 19, 20; Table 1). Macronucleus nodules widely apart, but connected by a fine strand recognizable only in protargol preparations; anterior nodule at level of proximal end of adoral zone of membranelles, shorter by 5 µm than posterior nodule; nodules bluntly to elongate ellipsoidal (1.3–5:1), anterior nodule on average bluntly ellipsoidal (1.7:1), posterior elongate ellipsoidal (2.4:1), both studded with small nucleoli. Micronuclei attached to macronucleus nodules, well recognizable *in vivo*, but not impregnable with protargol, not even in dividing cells. Contractile vacuole at level of proximal end of adoral zone of membranelles, that is, distinctly above mid-body at left margin of cell, with lacunar collecting canals (Fig. 1); opening sometimes recognizable in protargol preparations (Fig. 57). Feeds on a variety of items, such as starch grains from the squashed kernels added to the culture; small rotifers digested in vacuoles up to 60 µm across; heterotrophic and autotrophic flagellates (*Polytomella*, *Rhodomonas*); and middle-sized ciliates (*Colpidium kleini*, *Cyrtolophosis mucicola*, *Vorticella* sp., division cysts of *Colpoda steinii*), while larger species (*Paramecium aurelia*) are rejected. *Polytomella* and starch grains were preferred in cultures.

Cells golden yellow to brown orange in the dissecting microscope and with beautiful golden sheen under oblique dark-field illumination. Colour caused by a rather intense orange colouration of the cytoplasm, especially in oral area, and numerous citrine cortical granules, forming narrow strands ventrally and dorsally. Cortical granules ellipsoid to obovate, attached with broad end (Figs 7, 34), about 2 × 1.3 µm in size, become deeply orange-coloured and ~ 1.5 µm across when detached from cortex or touched by coverslip (Figs 7, 32), arranged in complex pattern: (i) between adoral membranelles and within cirral rows (Figs 3–5, 32); (ii) left underneath frontal cirri, forming brick-shaped aggregates each composed of four to six granule pairs

◀◀

Figs 1–13. *Neokeronopsis* (*Afrokeronopsis*) *aurea* from life (1–7, 9, 12, 13) and after protargol impregnation (8, 10, 11). **1**, **2**, **9** – ventral and lateral view of a representative specimen. The scheme (9) shows main structures of the oral area, especially the roundish buccal depression (arrow) in the anterior region of the buccal cavity. Note the adoral zone of membranelles whose right portion almost approaches the level of the buccal vertex; **3–6** – cortical granulation in frontal area, on ventral side, in transverse cirral row, and on dorsal side; **7** – cortical granules are about 2 µm long, oval, and citrine; when disturbed, they become orange-coloured globules about 1.5 µm across; **8** – fibre system associated with ventral cirri in mid-body; **10a** – schematized shape of adoral zone of membranelles, with frontal membranelles forming a long tail; **10b** – size and structure of ventral adoral membranelles above and in mid-level of buccal cavity; **11** – fibre system of dorsomarginal kineties; **12**, **13** – resting cyst in optical section and surface view, showing polygonal facets produced by flat ridges. AM – adoral membranelles, AZM – adoral zone of membranelles, BL – buccal lip, C – cortex, DB – dorsal bristles, F – fibres, FC – frontal cirral corona, G – cortical granules, IL – inner layer, LMR – left marginal row, MVR – midventral rows, OL – outer layer, PF – pharyngeal fibres, R – ridge, RMR – right marginal row, SC – scutum, TC – transverse cirral row. Scale bars: 100 µm (1, 2, 9), 20 µm (8), 10 µm (10), 25 µm (11), 50 µm (12, 13).

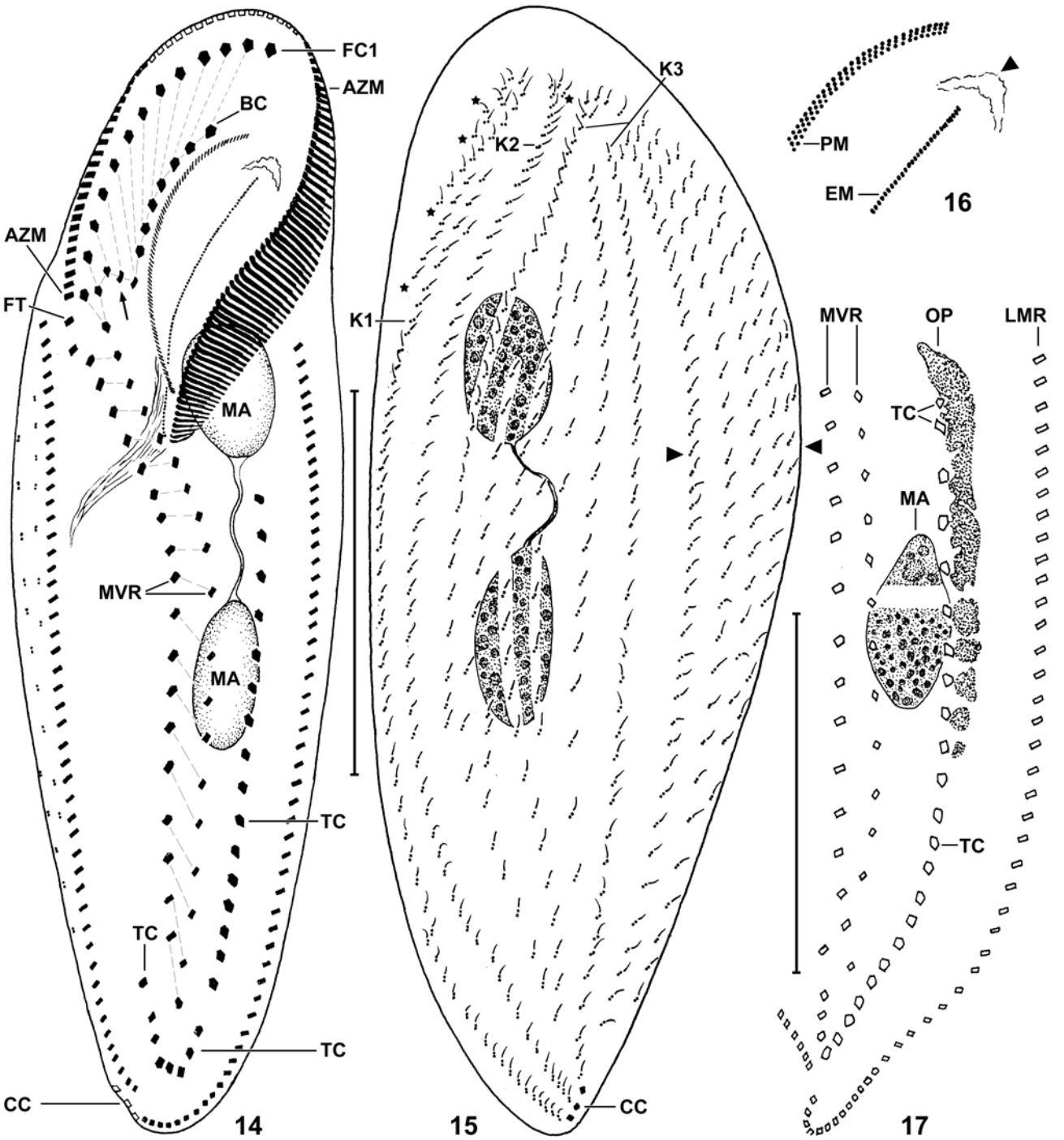

Figs 14–17. *Neokeronopsis* (*Afrokeronopsis*) *aurea*, infraciliature after protargol impregnation. **14**, **16** – ventral view. Pairs of midventral cirri are connected by hatched lines, showing that the frontal and buccal row consist of midventral cirri, except of the first frontal cirrus which is generated by the undulating membranes (Figs 43–45). Note the long adoral zone of membranelles, the long row of transverse cirri, the two frontoterminal cirri, and the hook of the buccal cirral row (arrow). The detail, which is from the same specimen, shows the paroral membrane composed of short, oblique rows of basal bodies. The triangle marks a wrinkled structure corresponding to the site of the buccal depression (cp. Fig. 9); **15** – dorsal view. Triangles delimit dorsomarginal rows, asterisks denote anterior fragments of dorsal kineties 1and 2; **17** – very early divider. The oral primordium develops along the anterior half of the transverse cirral row. AZM – adoral zone of membranelles, BC – buccal cirral row, CC – caudal cirri, EM – endoral membrane, FC1 – first frontal cirrus, FT – frontoterminal cirri, K1–K3 – dorsal kineties, LMR – left marginal row, MA – macronucleus nodules, MVR – midventral rows, OP – oral primordium, PM – paroral membrane, TC – transverse cirral row. Scale bars: 100 μm.

(Figs 3, 28); (iii) between cirral rows, forming narrow strands of scattered granules (Fig. 4); (iv) around dorsal bristles, thus imitating dorsal kinety pattern (Fig. 6); and (v) lacking between transverse cirral row and left marginal row.

Cirral pattern urostylid (Berger 2006), frequently with small irregularities, such as breaks and/or some supernumerary cirri; frontal cirri and adoral membranelles form an impressive, apical corona (Figs 1, 14, 18, 19, 25, 38b; Table 1); cirri associated with complex fibre system very similar in all rows, except of transverse cirri lacking laterally extending fibres (Fig. 8). Most cirri of ordinary thickness and length (18–23 µm), except of enlarged frontal, buccal, and transverse cirri; distances of cirri within rows rather constant, except of narrowly spaced cirri in rear region of marginal rows; thickness of cirri gradually decreasing from anterior to posterior, especially in marginal rows. Both marginal rows commence slightly above level of buccal vertex; right row almost straight ending subterminally, left row J-shaped curving around body end almost touching right row; gap between right and left row dorsally occupied by three inconspicuous, obliquely spread caudal cirri. Midventral rows about 7 µm apart in mid-body, cirri of right row visibly thicker than those of left, extend slightly obliquely and sigmoidally from right anterior end of body to near posterior end; with distinct irregularity at level of right end of adoral zone of membranelles, where rows commence to spread in a frontal corona and a hook-shaped buccal row with long portion of hook extending along right margin of buccal cavity (Figs 1, 14, 25, 38b); first frontal cirrus produced by the undulating membranes, frontal bow thus contains one cirrus more than buccal bow. Two inconspicuous frontoterminal cirri underneath right end of adoral zone of membranelles and close to right midventral row. Transverse cirri extraordinary because thick and about 30 µm long *in vivo*; arranged in a long, J-shaped row commencing underneath level of buccal vertex and extending subterminally around last midventral cirri, thus ending right of cell's midline (Figs 1, 14, 18, 19, 25, 38b; Table 1).

Dorsal bristles 4–5 µm long *in vivo*, densely spaced within rows, except of central body area occupied by loosely ciliated kinetofragments; encaged by long fibres in fusiform pattern, fibres especially distinct in dorsomarginal kineties. Bristle pattern complex and thus appearing fairly disordered at first glance, forms an average of 14 rows originating by different processes described in the ontogeny section (Figs 6, 11, 14, 15, 19, 20, 25, 26): (i) rows 1–3 in left third of cell, ontogenetically active and almost as long as body, i.e., commence subapically and end posteriorly left of midline with an inconspicuous caudal cirrus each; (ii) rows 1–3 fragmented in anterior portion, especially row 1; (iii) row 3 with multiple posterior fragmentation, producing about seven loosely ciliated kineties extending in middle body third and shortened anteriorly and posteriorly, except of ordinarily ciliated left and right row; (iv) in right body third about six dorsomarginal kineties decreasing in length from left to right.

Oral apparatus conspicuous due to the huge adoral zone of membranelles occupying almost 40% of body length and extending tail-like posteriorly on right body margin (Figs 1, 9, 14, 18–20, 25, 26, 38b; Table 1; for terminology, see Foissner and Al-Rasheid 2006). Adoral zone thus inverted U-shaped, respectively, narrowly spoon-shaped in plane projection (Fig. 10a); right half of U (spoon-handle) on right body margin, composed of minute, 3–5 µm long membranelles gradually increasing to 16–23 µm in left half, that is, at level of buccal cavity, and then gradually decreasing again to 3–5 µm in proximal region of zone covered by an inconspicuous buccal vertex. Membranelles of usual structure, i.e., exactly as described for *Sterkiella histriomuscorum* by Augustin and Foissner (1992), membranellar cilia, however, up to 20 µm long and highly differentiated (Figs 18, 30, 31, 33, 35, 36): (i) length of cilia greatly increases from right to left; (ii) cilia of row 1 acicular and distinctly longer than those of rows 2 and 3; (iii) cilia of rows 2 and 3 with obtuse distal end; (iv) row 4 consists of only three minute cilia with rounded distal end; (v) rightmost cilia of ventral membranelles differentiated to up to 10 µm long, "lateral membranellar cilia" *in vivo* covered by the buccal seal and extending to right wall of buccal cavity, in scanning electron microscopic preparations usually appearing as a highly disordered stripe of cilia (Figs 18, 30, 31).

Buccal cavity and undulating membranes basically of ordinary size and structure. However, the general appearance resembles a mixture of the *Oxytricha* and *Cyrtohymena* type because the cavity is rather large and deep, the endoral membrane extends obliquely across the cavity, and the buccal depression appears as a strongly curved elongation of the paroral membrane which, however, is not curved anteriorly (Figs 1, 9, 14, 18, 19, 25, 27–30; Table 1). Buccal depression circa 15 µm across *in vivo* and gradually deepening to about

5 µm, at anterior end of endoral membrane, left third covered by a hyaline plate possibly belonging to the buccal lip or buccal seal; proximal margin slightly tuberculate because touching anterior end of fibre bundle underneath endoral membrane; appears as a rather distinct, bright area *in vivo* (Figs 1, 28, 29); as a wrinkled,

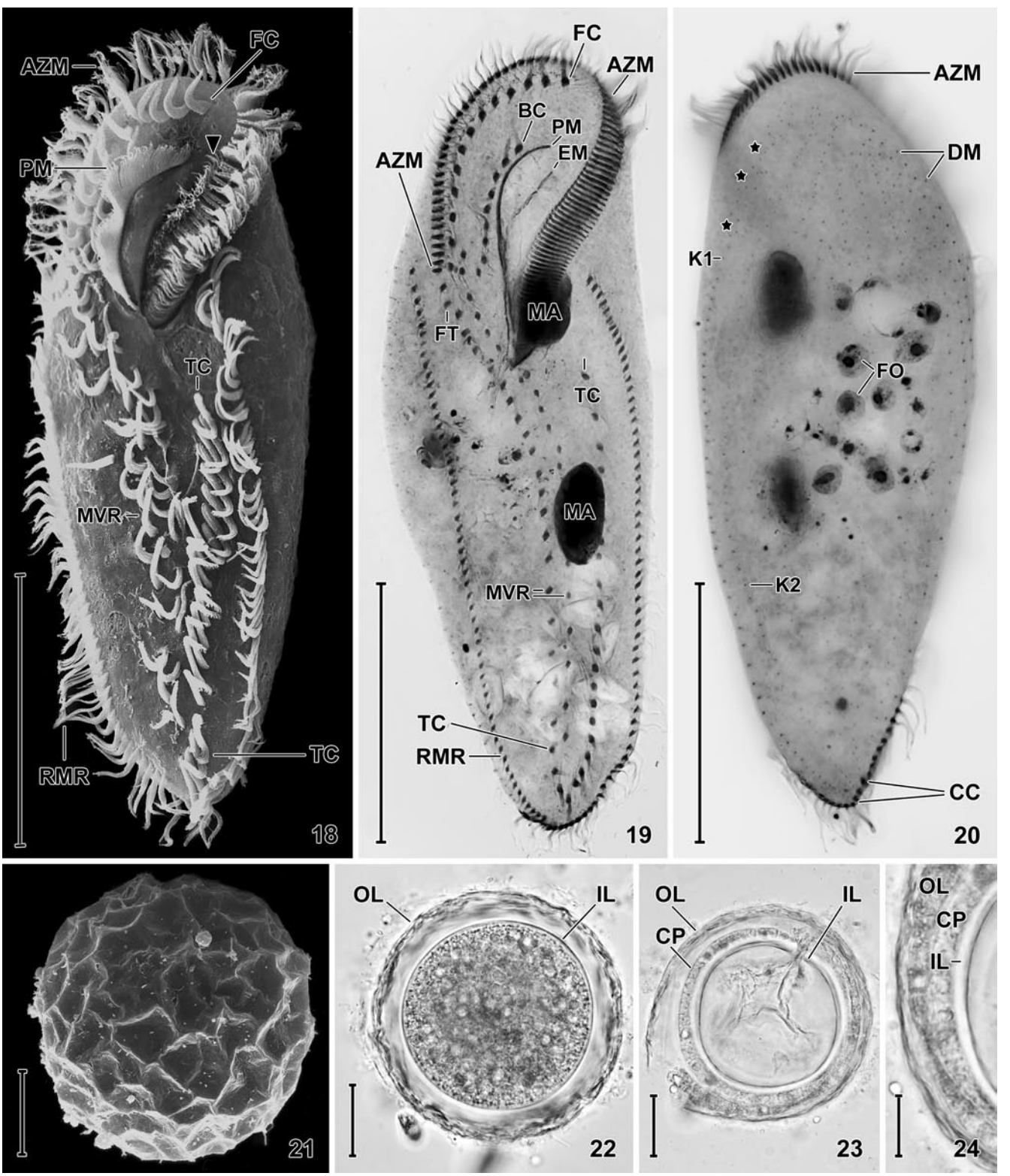

almost invisible structure in protargol preparations (Figs 14, 19, 25, 27); and is invisible in the scanning electron microscope because covered by the buccal seal (Figs 18, 30). Buccal seal usually broken at left margin of buccal cavity, partially exposing endoral and lateral membranellar cilia (see above). We could not decide whether there is an upper and a lower seal or only the upper one.

Paroral membrane on base of the about 3 μm wide, inconspicuous buccal lip; distinctly curved but not extending to adoral zone of membranelles anteriorly, as in *Cyrtohymena*; polystichad, i.e., massive because consisting of very narrowly spaced, oblique kineties, each composed of three to four up to 20 μm long cilia decreasing to 10 μm and less in end regions of membrane (Figs 1, 9, 14, 16, 18–19, 25, 27, 30, 37; Table 1). Endoral membrane extends more or less obliquely across buccal cavity, posterior third rather sharply curved and intersecting optically with paroral membrane; composed of very narrowly spaced mono- or dikinetids; underlayed by a thick fibre bundle performing undulating movements under slight coverslip pressure. Pharyngeal fibres inconspicuous, extend obliquely backwards (Figs 1, 9, 14, 16, 19, 25, 27, 30; Table 1).

Resting cyst

Resting cysts conspicuous because 116 μm across on average ($\bar{x}$ 116.4, M 120.0, SD 5.0, SE 1.8, CV 4.3, Min 105, Max 120, n 14), invariably globular, dark at × 40––100, brown at higher magnifications, consist of two distinct layers (Figs 12, 13, 21–24): outer layer 25 μm thick on average ($\bar{x}$ 24.6, M 25.0, SD 3.9, SE 1.1, CV 15.8, Min 18, Max 30, n 14), hyaline and without any stratification, colourless, stains red with methyl green-pyronin, surface grown with bacteria and polygonally faceted by 1–2 μm high ridges distinct only in the scanning electron microscope; inner layer about 2 μm thick, compact and colourless. Cytoplasm studded with three kinds of inclusions: (i) colourless lipid droplets 2–10 μm across, usually 4–8 μm; (ii) orange-coloured, bright granules 0.5–3 μm across, providing the squashed cyst contents with a reddish sheen in interference contrast; (iii) colourless (crystalline?) granules about 1 × 0.7 μm in size. Unfortunately, we did not note whether the macronucleus nodules remain separate or fuse.

Ontogenesis of *N.* (*Afrokeronopsis*) *aurea*

Many well-impregnated dividers were found in the protargol slides. Thus, each of the stages depicted has been seen in at least three specimens. The description is very detailed because the diagnoses contain sophisticated ontogenetic features and further research might show the need to include even more. We include also the ontogenetic comparison with *N.* (*N.*) *spectabilis*, as far as this is possible from the rather incomplete descriptions of Warren *et al*. (2002) and Wang *et al*. (2007).

Cell fission, nuclear apparatus, and parental cirri: Cell fission and division of the nuclear apparatus proceed as in most other oxytrichids and urostylids (for reviews, see Berger 1999, 2006). Thus, we refer to the figures and the detailed figure explanations. A considerable portion of the parental cirri and dorsal bristles is still recognizable in early and even late post-dividers (Figs 59–61). Finally, however, the complete parental ciliature is resorbed and rebuilt, except of the adoral zone of membranelles.

Oral apparatus: The oral primordium develops close to the left of about 10 anterior transverse cirri, most of which are soon incorporated into the anlagen field (Fig. 17). The bluntly conical anterior end of the oral primordium extends slightly above the transverse cirral row, but never reaches the buccal vertex (Fig. 17). In contrast to *Neokeronopsis* (*N.*) *spectabilis* (Wang *et al*. 2007), postoral anlagen fields are lacking, an important difference checked in four very early dividers. Next, a loose array of basal bodies grows out from the right anterior end of the oral primordium, soon forming minute rows of dikinetids (Fig. 39c). This small array develops to the undulating membranes and contributes to the primordium of the midventral rows.

◀◀

Figs 18–24. *Neokeronopsis* (*Afrokeronopsis*) *aurea* in the scanning electron microscope (18, 21), after protargol impregnation (19, 20), and from life (22–24). **18**, **19** – ventral views showing overall organization. Triangle in Figure 18 marks the lateral membranellar cilia of the adoral membranelles; **20** – dorsal view. Asterisks denote anterior fragments of dorsal kinety 1; **21**, **22** – surface view and optical section of resting cysts; **23**, **24** – squashed resting cyst showing wall details. Some cytoplasm extends between inner and outer layer showing that the latter is not very compact. AZM – adoral zone of membranelles, BC – buccal cirral row, CC – caudal cirri, CP – cytoplasm, DM – dorsomarginal kineties, FC – frontal cirral corona, FO – food inclusions, FT – frontoterminal cirri, IL – inner layer, K1, K2 – dorsal kineties, MA – macronucleus nodules, MVR – midventral rows, OL – outer layer, PM – paroral membrane, RMR – right marginal row, TC – transverse cirral row. Scale bars: 100 μm (Figs 18–20), 30 μm (21–23), 10 μm (24).

The fully developed oral primordium extends along the left side of the anterior two thirds of the transverse cirral row, and protomembranelles, each composed of two rows of basal bodies, develop at the right margin of the anterior third of the oral primordium. Concomitantly, the loose array of basal bodies described above enlarges

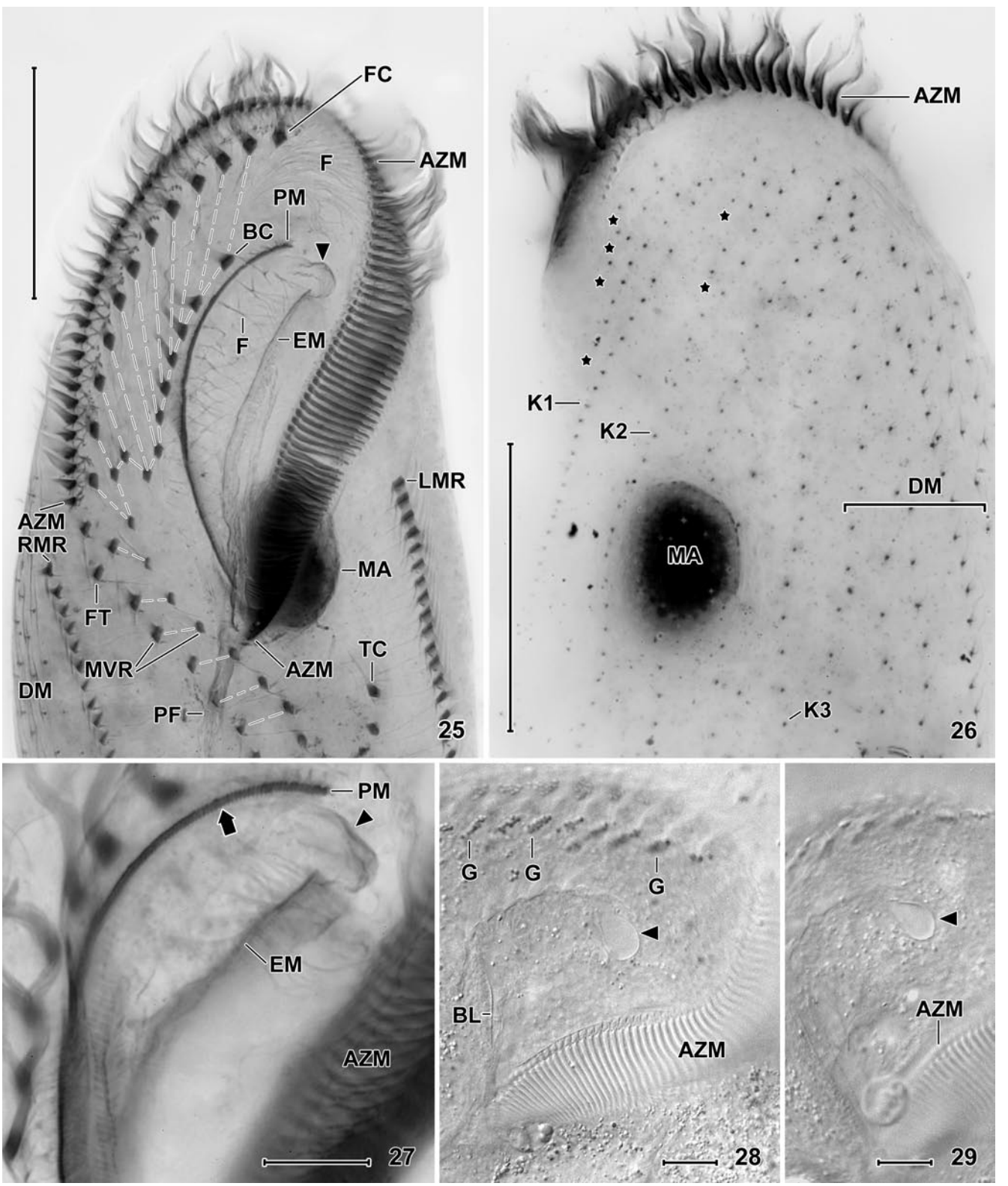

greatly and extends posteriorly to meet an anlagen field originating from the midventral rows (Figs 39a, 42). Slightly later, protomembranelles have formed in the anterior half of the oral primordium and basal bodies begin to segregate for the new undulating membranes; further, the parental undulating membranes are dissolving (Fig. 40). During all these processes, the proximal end of the parental adoral zone and the distal end of the oral primordium are clearly separate, while both almost touch in *N.* (*N.*) *spectabilis* (Wang *et al*. 2007).

In mid-dividers, the oral primordium develops to a long ribbon with the anterior third sharply curved rightwards (Figs 44, 45). At the right side of the straight portion extends a thick streak of anarchic basal bodies, later forming the undulating membranes. The first frontal cirrus segregates from the right anterior end of the streak. The disintegration of the parental undulating membranes and pharyngeal fibres has been completed, leaving a narrow, strongly flattened buccal cavity and a thick streak of anarchic basal bodies right of the straight portion of the adoral zone. The streak of anarchic basal bodies develops by multiplication of basal bodies from the parental membranes, i.e., cirri are not involved. The first frontal cirrus is formed as described for the opisthe. The parental adoral zone of membranelles is inherited unchanged. All these processes are highly similar to those described in *N.* (*N.*) *spectabilis* (Warren *et al*. 2002, Wang *et al*. 2007), except of the anterior portion of the adoral zone which is much less curved than in *N.* (*A.*) *aurea*.

In late and very late dividers, where the fission furrow becomes recognizable, the adoral membranelles and the membranellar zone obtain their definite structure and shape, i.e., a third and fourth row of basal bodies are added to the individual membranelles and the distances between the membranelles increase in the anterior third of the zone, forming the long membranellar tail typical for this species (Figs 1, 10a, b, 14, 46–48). In both, the proter and opisthe, the two undulating membranes have formed from the anarchic streak of basal bodies described above. Interestingly, the developing membranes do not extend side by side, as in many other hypotrichs, but optically intersect from the beginning in the posterior quarter; this is also recognizable in *N.* (*N.*) *spectabilis* (Warren *et al*. 2002). Later, the intersecting area migrates to the mid of the membranes (Figs 47, 48). This part of the oral ontogenesis appears highly similar in *N.* (*N.*) *spectabilis* and *N.* (*A.*) *aurea*. Unfortunately, neither Warren *et al*. (2002) nor Wang *et al*. (2007) described the further development of the oral apparatus, that is, the origin of the buccal cavity and buccal depression (if present at all!).

In early post-dividers, the oral apparatus is quite similar to that of very late dividers (cp. Figs 48, 59), although the undulating membranes intersect more distinctly. Only in late post-dividers develop the pharyngeal fibres and the buccal depression as well as a typical cyrtohymenid oral apparatus with a deep buccal cavity and a strongly curved paroral membrane which now extends obliquely across the bottom of the buccal cavity (Fig. 61). Interestingly, the curvature of the paroral becomes flatter and thus *Oxytricha* – like in the fully grown specimens (cp. Figs. 14, 61).

Wang *et al*. (2007) emphasize the unique position of the early oral primordium in *N.* (*N.*) *spectabilis*: "Uniquely, the oral primordium originates below the anteriormost transverse cirrus, which is in contrast to almost all other stichotrichous ciliates in which the oral primordium originates anterior to the transverse cirri or even near the ventral cirri". However, this is not correct. Identical patterns are found in many oxytrichids, for instance, in *Onychodromopsis flexilis* (Petz and Foissner 1996) and *Sterkiella cavicola* (Foissner *et al*. 2002) as well as in some urostylids, for instance, *Pseudoamphisiella lacazei* and *Holosticha bradburyae* (for reviews, see Berger 1999, 2006). It appears that the early oral primordium usually extends along some anterior transverse cirri when these are numerous and form a row extending to mid-body. However, the oral primordium is indeed important in this group of species

◀◀

Figs 25–29. *Neokeronopsis* (*Afrokeronopsis*) *aurea* from life (28, 29) and after protargol impregnation (25–27). **25**, **27–29** – ventral views showing oral area. Hatched lines connect pairs of midventral cirri (cp. Fig. 14). The arrow (27) marks the oblique kineties composing the paroral membrane. *In vivo*, the buccal depression appears as a bright spot (triangles) shown in two focal planes in Figures 28 and 29 taken from a squashed specimen; **26** – dorsal view of anterior body portion, showing the fragmented kineties 1 and 2 (asterisks). AZM – adoral zone of membranelles, BC – buccal cirral row, BL – buccal lip, DM – dorsomarginal kineties, EM – endoral membrane, F – fibres, FC – frontal cirral corona, FT – frontoterminal cirri, G – cortical granules, K1–K3 – dorsal kineties, LMR – left marginal row, MA – macronucleus nodules, MVR – midventral rows, PF – pharyngeal fibres, PM – paroral membrane, RMR – right marginal row, TC – transverse cirri. Scale bars: 50 μm (Figs 25, 26), 10 μm (27–29).

because there are three anlagen fields in *N.* (*N.*) *spectabilis* while only one in *N.* (*A.*) *aurea* (see above and diagnoses of subgenera).

Ventral cirral pattern: In *N.* (*A.*) *aurea*, the midventral complex (Berger 2006) contains the midventral rows and their derivates, i.e., the frontal cirral corona, the buccal and transverse cirral row, and the frontoterminal cirri. The genesis of the midventral complex is highly similar in *N.* (*A.*) *aurea* and *N.* (*N.*) *spectabilis*, suggesting to summarize the relevant processes in a concise paragraph.

(i) The midventral complex develops independently, but concomitantly, in proter and opisthe (Figs 39a, c, 41, 42). (ii) Basically, the midventral complex is generated

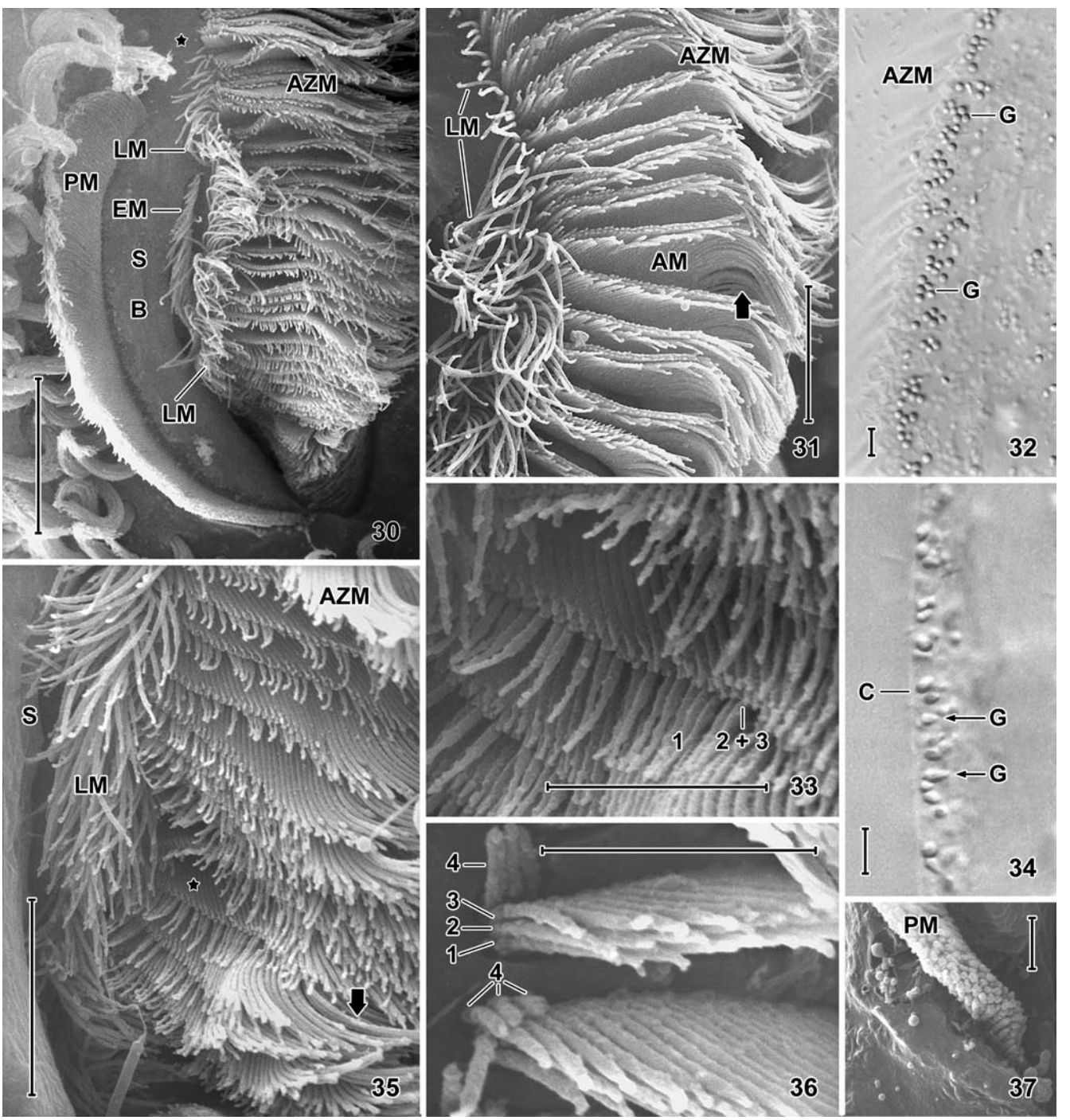

by the parental midventral rows (Figs 39a, c, 41, 42). In the proter, the complex originates from the buccal cirral row which is, in fact, the anterior portion of the left midventral row (Figs 47, 48, 59, 61); likely, one cirrus of the right row is involved because it is dissolved. The opisthe midventral complex is generated mainly by some cirri of the midventral rows (Fig. 39a) and, to a smaller part, by an anterior outgrowth of the oral primordium, possibly generating the undulating membranes (Fig. 39c). (iii) Short, oblique cirral streaks develop in the midventral anlagen and produce three long cirral rows each in proter and opisthe, a highly characteristic pattern becoming recognizable in mid-dividers (Figs 44, 45). The number of cirral streaks determines the number of cirral pairs in the new midventral complex. There is no indication, how the number is controlled. However, some cirri in the anterior region of the proximal anlagen row, which becomes the transverse cirral row, do not assemble completely and soon become resorbed (Figs 44, 45).Thus, there are more midventral pairs than transverse cirri ($\overline{\times}$ 32 *vs.* 24). (iv) In late and very late dividers, the three cirral rows of the new midventral complex begin to migrate to their specific positions in both proter and opisthe; specifically, two frontoterminal cirri separate from the rear end of the cirral stripe and migrate anteriorly (Figs 44–48); the proximal row migrates left to become the transverse cirral row; and the anterior portion of the middle row curves leftwards to become the buccal cirral row, while the anterior portion of the distal row forms the frontal cirral corona (Figs 46–48). The final positioning of the cirri, i.e., the species-specific pattern is, however, hardly produced by active migration but by post-divisional growth. This is well recognizable in the buccal cirral row which becomes attached to the right margin of the buccal cavity because the cavity doubles its width during post-divisional growth (Figs 59, 61).

Marginal cirral rows: Basically, the marginal cirral rows reproduce as usual, that is, a primordium each develops in the proter and opisthe of early dividers (Figs 39a, 40). The primordia are produced by a single cirrus each, at least in the left row where the first cirrus and one cirrus in mid-body develop to an anlage each (Fig. 39b). All other parental marginal cirri are resorbed later. Anlagen formation commences slightly earlier in the right than in the left marginal row (Figs 39a, 40), but occurs concomitantly in proter and opisthe, while the opisthe's marginal anlagen appear later than those of the proter in *N.* (*N.*) *spectabilis* (Wang *et al*. 2007). Five to six dorsomarginal kineties develop right of the anterior end of the right marginal cirral primordia in early mid-dividers to late dividers (Figs 44, 45). The dorsomarginal kineties increase in length from left to right and migrate onto the dorsal side in late dividers (Figs 46–48).

Dorsal ciliature: The dorsal ciliature of *N.* (*A.*) *aurea* consists of three distinct parts (see descriptive section) and develops in the oxytrichid way, i.e., according to type IV (Foissner and Adam 1983), as already recognized by Warren *et al*. (2002) and Wang *et al*. (2007). However, there are several specializations showing that *N.* (*A.*) *aurea* represents a distinct subtype, viz., the multiple anterior fragmentation of kineties 1–3 and the kinety whirl associated with the posterior fragmentation of kinety 3. Both specializations have not been described in *N.* (*N.*) *spectabilis* (Warren *et al*. 2002, Wang *et al*. 2007), but it is uncertain whether they are lacking or have been overlooked (for details, see reinvestigation of *N. spectabilis* below).

◀◀

Figs 30–37. *Neokeronopsis* (*Afrokeronopsis*) *aurea*, cortical granules *in vivo* (32, 34) and oral apparatus in the scanning electron microscope (30, 31, 33, 35–37). **30**, **37** – overview of oral apparatus. Note the buccal seal (S) which is very fragile and covers the buccal cavity. Thus, the cavity and the structures within the cavity cannot be seen in the scanning electron microscope, viz., the roundish buccal depression (Figs 9, 28), the endoral membrane (Figs 25, 27), and the lateral membranellar cilia (LM) which commence close above the buccal cavity (asterisk); however, the latter and the distal end of the endoral cilia become visible due to a preparation – induced break of the seal at the left margin. The paroral membrane is thick because it is composed of short, oblique ciliary rows from the anterior to the posterior (37) end; **31**, **33**, **35**, **36** (33 is a higher magnification of 35, asterisk) – details of ventral (buccal) adoral membranelles. The lateral membranellar cilia (LM), which are usually rather disordered, increase in length from anterior to posterior (31) and are absent above the buccal cavity (36). The individual membranelles are composed of four rows (36) of specialized cilia: row 4 consists of three cilia which are about 2 µm long in the frontal membranelles (36) and increase to about 15 µm when becoming lateral membranellar cilia along the buccal cavity (31, 35); rows 3 and 2 have moderately long, obtuse cilia elongating leftwards to up to 10 µm (35); and row 1 has long, acicular cilia increasing in length leftwards to up to 20 µm *in vivo* (31, 35, arrows); **32**, **34** – cortical granules are orange-coloured and about 1.5 µm across when disturbed (32), while citrine, obovate and about 2 µm long when undisturbed (34). AM – adoral membranelles, AZM – adoral zone of membranelles, B – buccal cavity, C – cortex, EM – endoral membrane, G – cortical granules, LM – lateral membranellar cilia, PM – paroral membrane, S – buccal seal, 1, 2, 3, 4 – ciliary rows of adoral membranelles. Scale bars: 20 µm (Fig. 30), 10 µm (31, 35), 5 µm (32–34, 36), 2 µm (37).

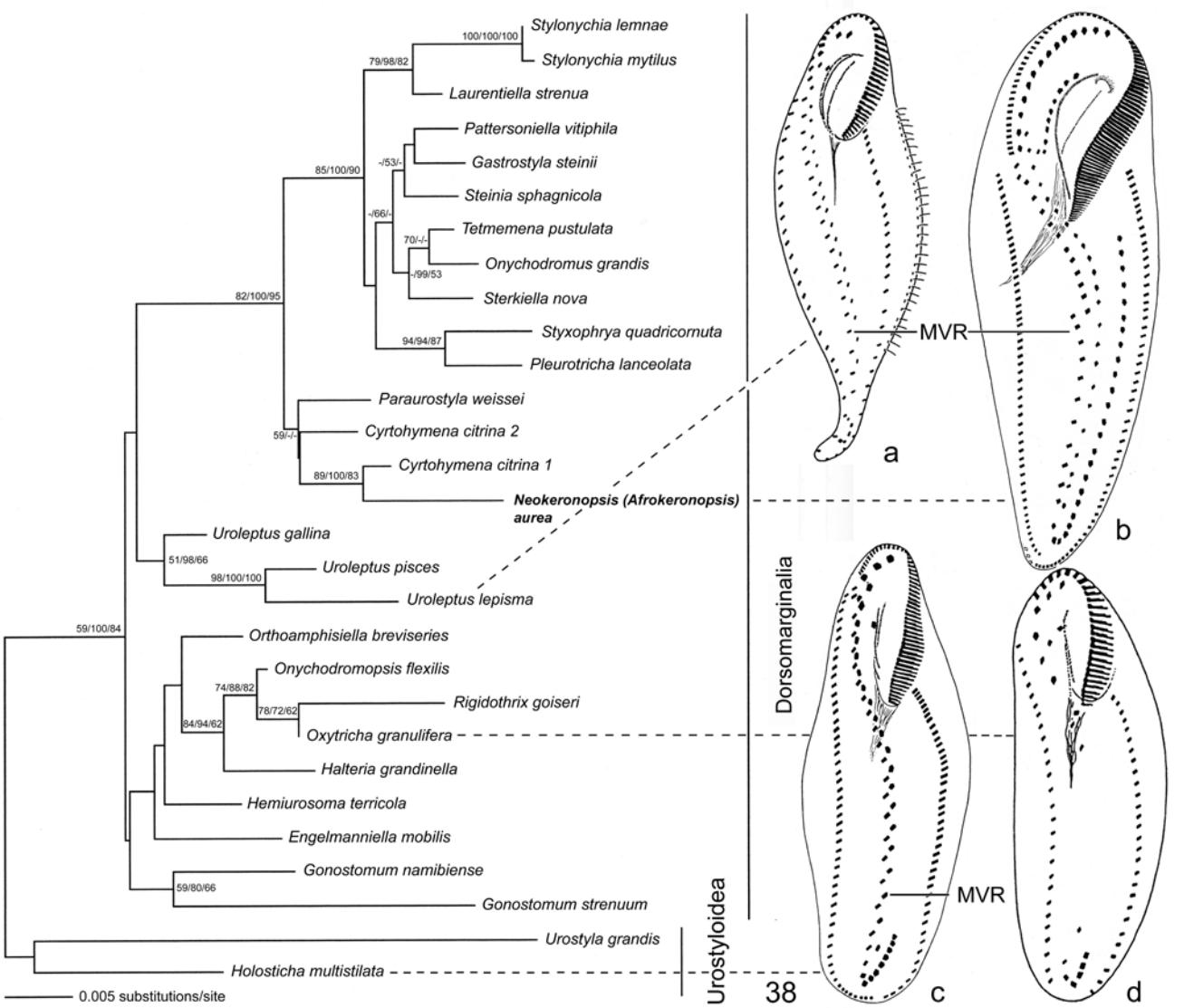

Fig. 38. Maximum likelihood tree of 18S rDNA sequences showing the position of *Neokeronopsis* (*Afrokeronopsis*) *aurea*. The tree was constructed by using a GTR+I+G DNA substitution model with the variable-site gamma distribution shape parameter (G) at 0.4635; the proportion of invariable sites at 0.8322; and base frequencies and a rate matrix for the substitution model as suggested by Modeltest (Akaike Information Criterion, AIC), based on 1,703 unambiguously aligned positions. ML and distance bootstrap values over 50% from an analysis of 1000 bootstrap replicates each (first and second number, respectively) and posterior probabilities over 50% of 751 bayesian trees (third number), are given at the respective nodes. *Neokeronopsis* (*Afrokeronopsis*) *aurea* branches within the *Cyrtohymena* cluster. However, *Cyrtohymena* has a very different cirral pattern composed of 18 frontal, ventral, and transverse cirri (Fig. 38d, *Oxytricha islandica*; from Berger and Foissner 1989). Thus, we propose that *Neokeronopsis* (*Afrokeronopsis*) *aurea* (Fig. 38b) is related to the oxytrichid genus *Pattersoniella* which also has midventral cirri producing the frontal and buccal cirral corona. The tree shows that midventral rows (MVR) evolved independently in at least four lineages: the Urostyloidea, e.g., *Holosticha* (38c, from Berger 2006); the core oxytrichs, viz., *Rigidothrix goiseri* (Foissner and Stoeck 2006); the uroleptids, e.g., *Uroleptus* (38a, from Berger 2006) and the stylonychine oxytrichs, e.g., *Neokeronopsis* (38b) and *Pattersoniella* (Berger 2006).

Ontogenesis of the dorsal ciliature commences within kinety 3, where a dikinetidal anlagen streak each develops above and underneath mid-body (Fig. 49). Then follow kineties 1 and 2 and all anlagen develop to long, dikinetidal streaks extending to the ends of the cell left of the parental bristle rows (Figs 50, 55). In

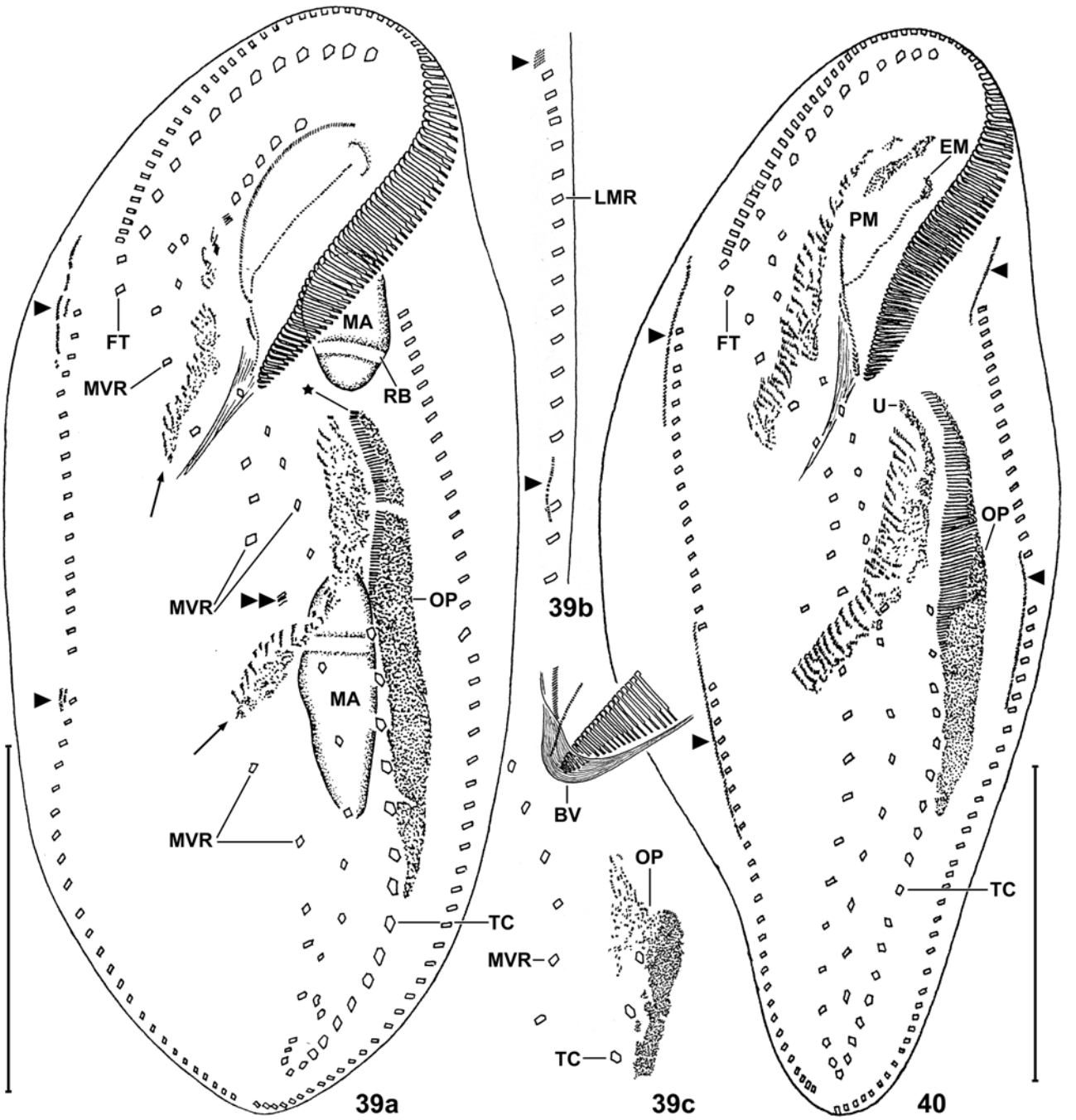

Figs 39, 40. *Neokeronopsis* (*Afrokeronopsis*) *aurea*, ventral views of very early (39c) and early dividers (39a, b, 40) after protargol impregnation. A very early division stage is also shown in Figure 17. **39a** – early divider showing that cirral anlagen (arrows) of proter and opisthe develop independently from and within the midventral rows; the proter anlage includes most buccal cirri, while the opisthe anlage includes basal bodies from the oral primordium (39c). Triangles mark the just appearing anlagen of the right marginal rows. The doubled triangle marks a dissolving midventral cirrus. The asterisk denotes organizing adoral membranelles along the right anterior margin of the oral primordium, where the transverse cirri have been resorbed; **39b** – the anlagen for the new left marginal rows develop from a single cirrus each at anterior end and in mid-body (triangles); **39c** – a very early divider following the stage shown in Figure 17. An anarchic field of basal bodies develops at the left anterior margin of the oral primordium and fuses with the anlagen produced by the midventral cirri (39a). Unlike *N.* (*N.*) *spectabilis* (Wang *et al*. 2007), there are no anlagen underneath the buccal vertex (BV); **40** – early mid-divider showing disorganizing parental undulating membranes (EM, PM) and anlagen (triangles) for the right and left marginal rows. New adoral membranelles are developing in the anterior half of the oral primordium. Note developing streaks in the cirral anlagen. BV – buccal vertex, EM – endoral membrane, FT – frontoterminal cirri, LMR – left marginal row, MA – macronucleus nodules, MVR – midventral rows, OP – oral primordium, PM – paroral membrane, RB – reorganization band, TC – transverse cirral row, U – anlage for the undulating membranes. Scale bars: 100 μm.

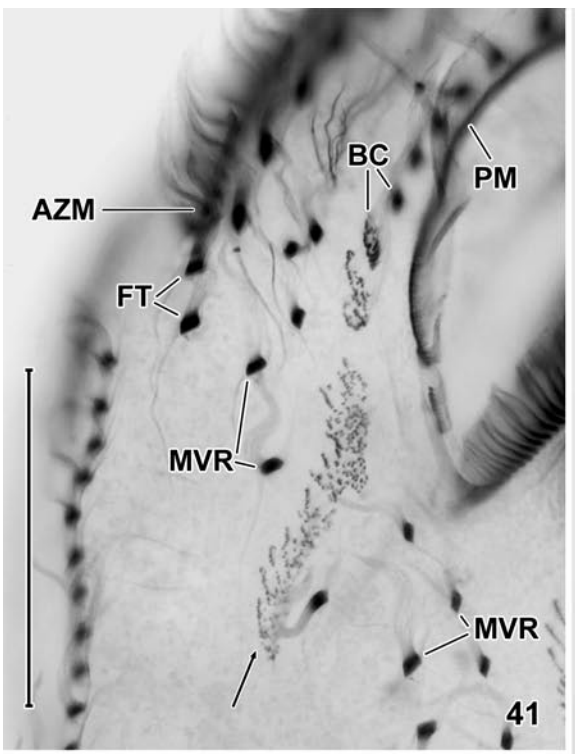

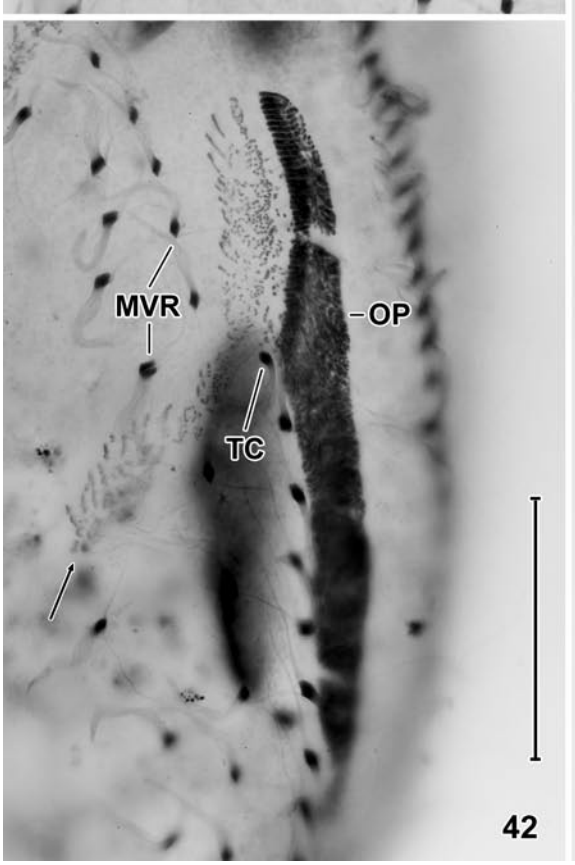

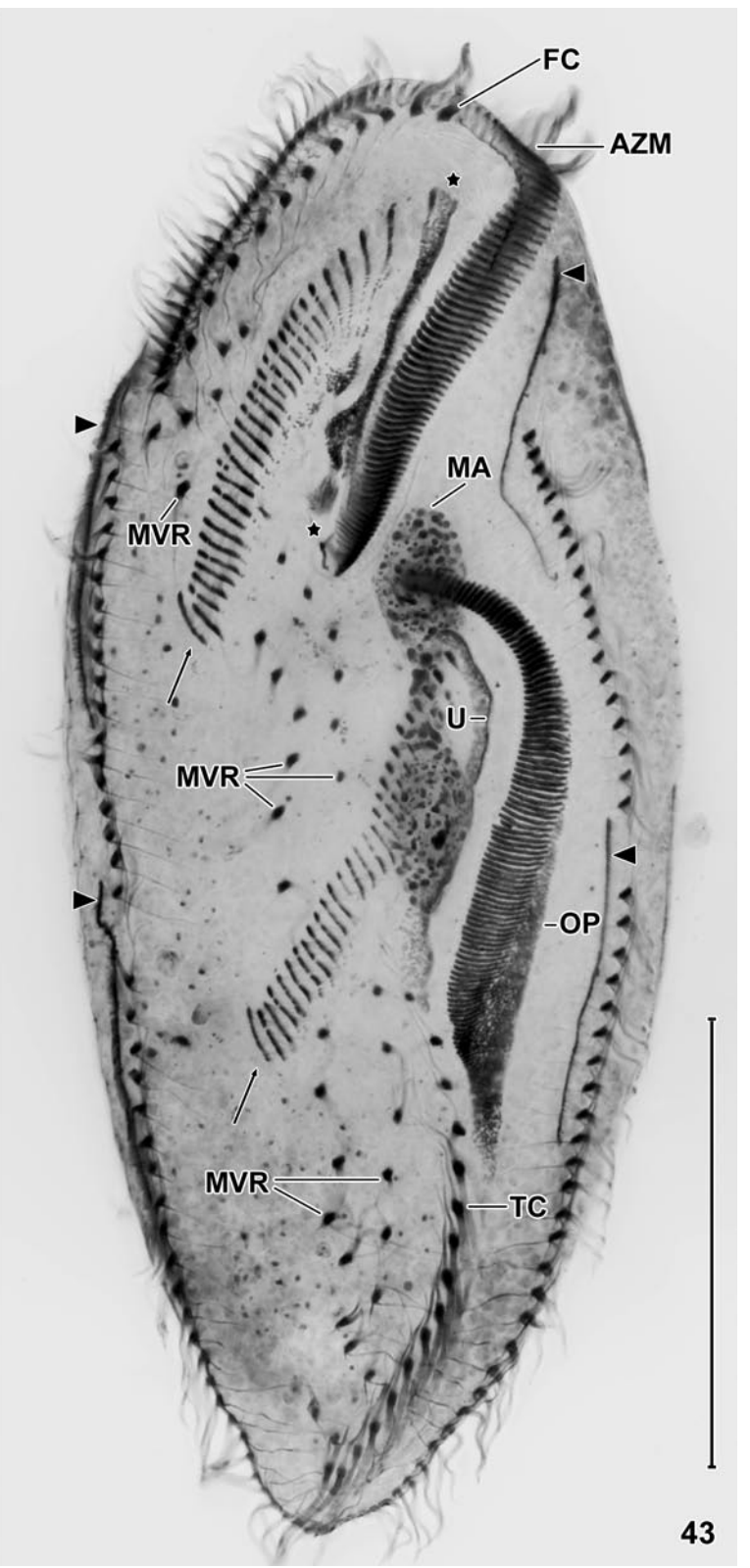

Figs 41–43. *Neokeronopsis* (*Afrokeronopsis*) *aurea*, ventral views of dividers after protargol impregnation. **41**, **42** – early divider with proter (41) and opisthe (42) cirral anlagen (arrows); **43** – middle divider with fusing macronucleus nodules. Arrows mark cirral anlagen; triangles denote anlagen for marginal rows; asterisks delimit the reorganizing parental undulating membranes. AZM – adoral zone of membranelles, BC – buccal cirri, FC – frontal corona, FT – frontoterminal cirri, MA – macronucleus, MVR – midventral rows, OP – oral primordium, PM – paroral membrane, TC – transverse cirral rows, U – developing undulating membranes. Scale bars: 100 µm (Fig. 43), 50 µm (41, 42).

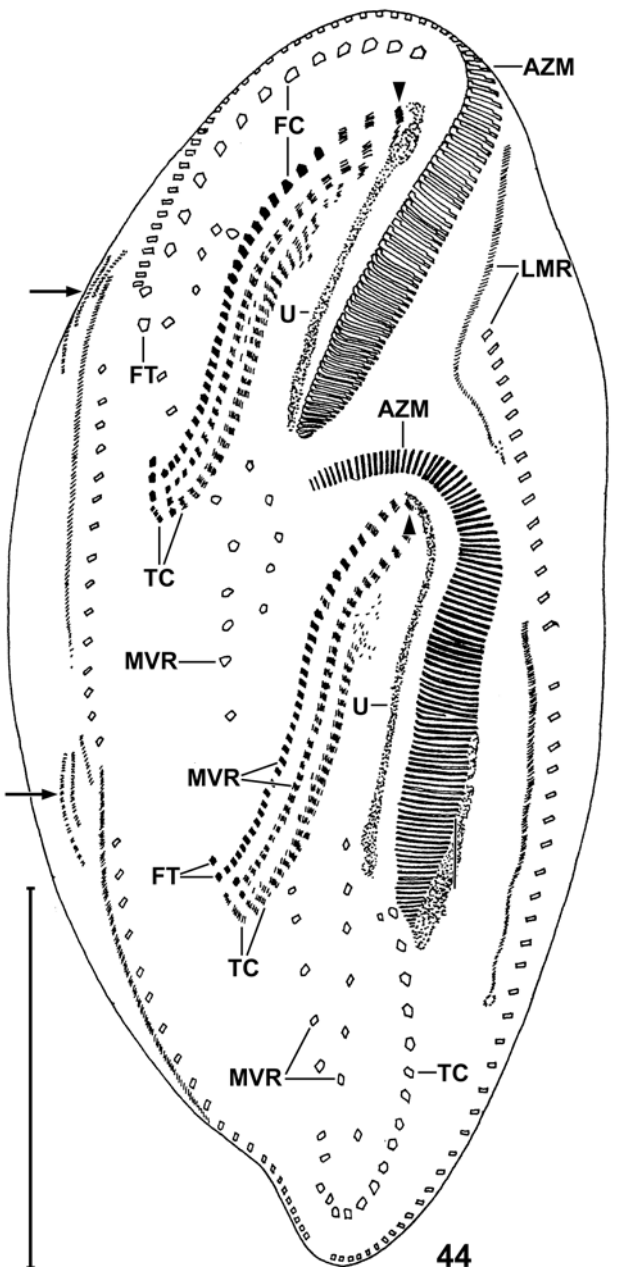

Fig. 44. *Neokeronopsis* (*Afrokeronopsis*) *aurea*, ventral view of a middle divider after protargol impregnation. In this stage, the macronucleus nodules have fused (Fig. 45) and the new cirri have segregated forming three conspicuous, sigmoidal rows each in proter and opisthe: the upper two rows will produce the new midventral rows, while the lower row will generate the transverse cirral row. The undulating membranes (U) are forming and have produced the first frontal cirrus (triangle). Arrows mark developing dorsomarginal kineties. AZM – adoral zone of membranelles, FC – frontal cirral coronas, FT – frontoterminal cirri, LMR – left marginal rows, MVR – midventral rows, TC – transverse cirral rows, U – undulating membranes. Scale bar: 100 μm.

early mid-dividers, a unique kinety whirl develops in the posterior third of kinety anlage 3, both in proter and opisthe (Figs 51, 57, 58). Although this event has not been described in *N.* (*N.*) *spectabilis*, we suppose that it occurs also in this species because the following stage is present in both, *N.* (*N.*) *spectabilis* and *N.* (*A.*) *aurea*: the whirl spreads and forms four to five short, sigmoidal, staggering kineties in mid-dividers (Fig. 52). Next, the staggering kineties increase in number by further fragmentation (Fig. 53) and then extend in the central third of the cell (Figs 54, 56) to form a fusiform bristle field in post-dividers (Fig. 60) and morphostatic specimens (Figs 15, 20, 26).

During the spread of the posterior fragments of kinety 3, another remarkable process begins not known from any other hypotrich: the anterior third of the newly formed kineties 1 and 2 as well as the leftmost fragment of kinety 3 commence to fragment, forming several short kineties in the broad anterior region of the cell (Figs 53, 54). This unique process is most distinct in kinety 1 and less distinct in kinety 3. When anterior and posterior fragmentation of kineties 1–3 have been completed, cell fission commences and the dorsomarginal kineties migrate onto the dorsal surface in late dividers (Fig. 54) and early post-dividers (Fig. 60). Thus, three main ontogenetic regions occur on the dorsal surface: the left third is occupied by kineties 1 and 2 and their anterior fragments; the middle third is occupied by kinety 3 and its posterior fragments; and the right third is filled with dorsomarginal kineties originating close to the right marginal row.

A caudal cirrus each develops at the posterior end of kineties 1–3 in late dividers (Fig. 53). As usual, the caudal cirrus of kinety 3 is produced by the rightmost fragment, while anterior fragmentation occurs in the leftmost fragment (Figs 53, 54). This fragmentation pattern suggests that kinety 3 is homologous to kineties 3 and 4 of the oxytrichids s. str. (for a review, see Berger 1999). *Neokeronopsis* (*N.*) *spectabilis* generates several caudal cirri in each kinety, a conspicuous difference used to define the subgenera *Neokeronopsis* and *Afrokeronopsis* as well as the species *spectabilis* and *aurea*.

Sequence analysis

The 18S rDNA sequence of *N.* (*A.*) *aurea* is 1,768 bp long and available under GenBank accession number EU124669. Comparing the *N.* (*A.*) *aurea* sequence to sequences from representative flexible and rigid hypotrichs identifies the flexible *Crytohymena citrina* (accession numbers AF508755, AY498653) as the closest

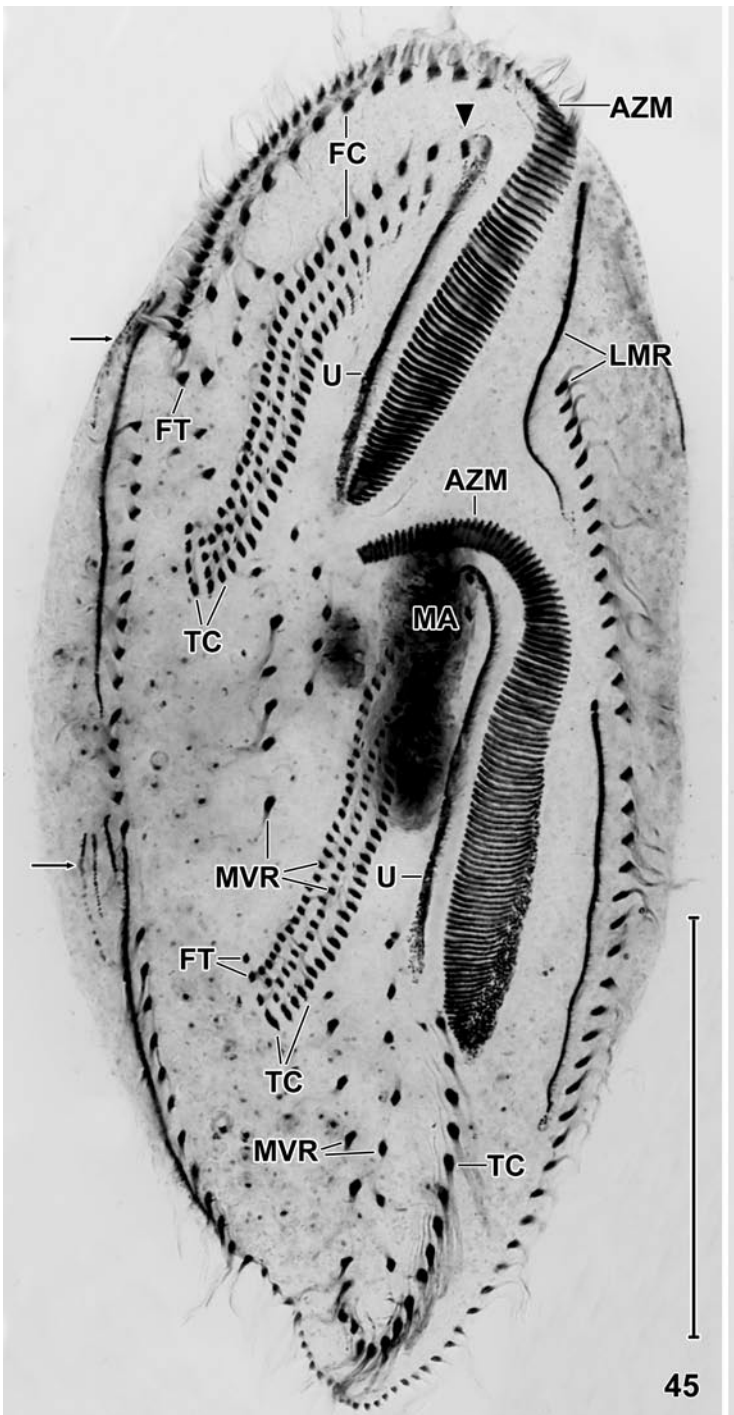

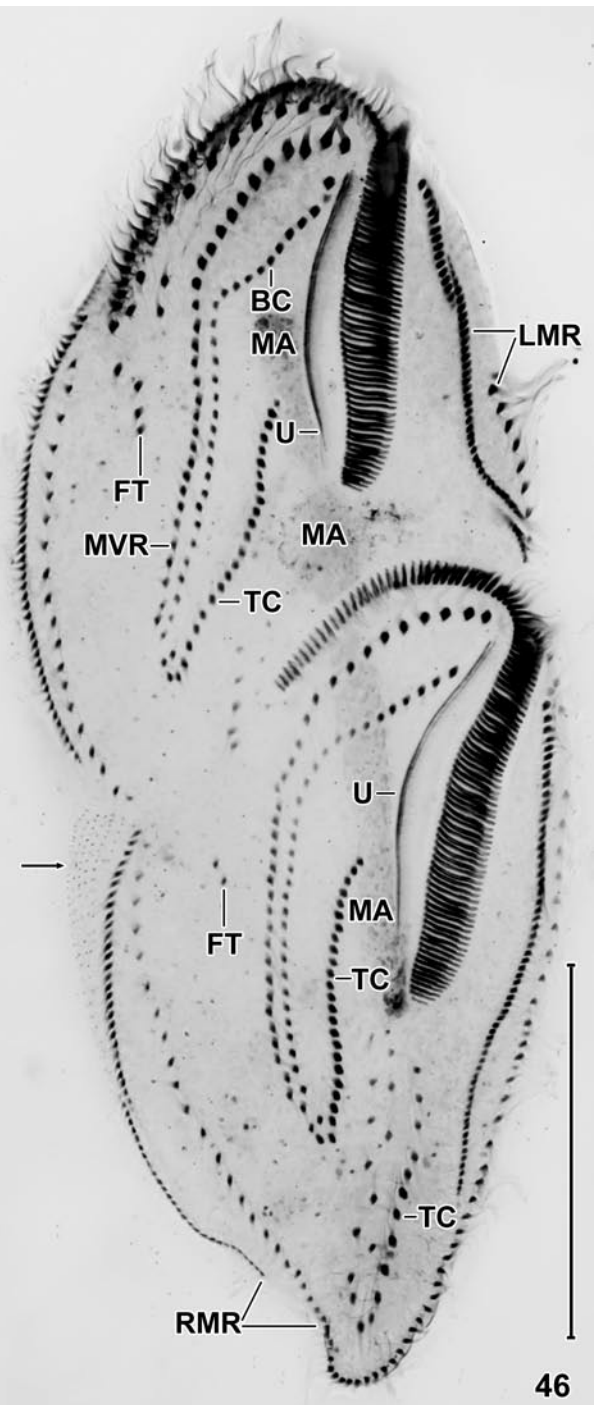

Figs 45, 46. *Neokeronopsis* (*Afrokeronopsis*) *aurea*, ventral views of dividers after protargol impregnation. **45** – middle divider, as shown in Figure 44. The macronucleus nodules have fused and the new cirri segregated within the anlagen, producing three conspicuous, sigmoidal rows each in proter and opisthe: the upper two rows will form the new midventral rows, while the lower row will generate the transverse cirral row. The undulating membranes (U) are organizing and have produced the first frontal cirrus (triangle). Arrows mark developing dorsomarginal kineties. **46** – late divider, as shown in Figure 47. The macronucleus elongated to a rod-shaped structure and the division furrow becomes recognizable. The new cirri are migrating to their specific positions, but not yet replaced the parental cirri. Note that the buccal cirri (BC) are part of the left midventral row, an unusual mode of producing buccal cirri. Arrow marks dorsomarginal kineties. AZM – adoral zone of membranelles, BC – buccal cirral row, FC – frontal cirral coronas, FT – frontoterminal cirri, LMR – left marginal rows, MA – macronucleus, MVR – midventral rows, RMR – right marginal rows, TC – transverse cirri, U – undulating membranes. Scale bars: 100 µm.

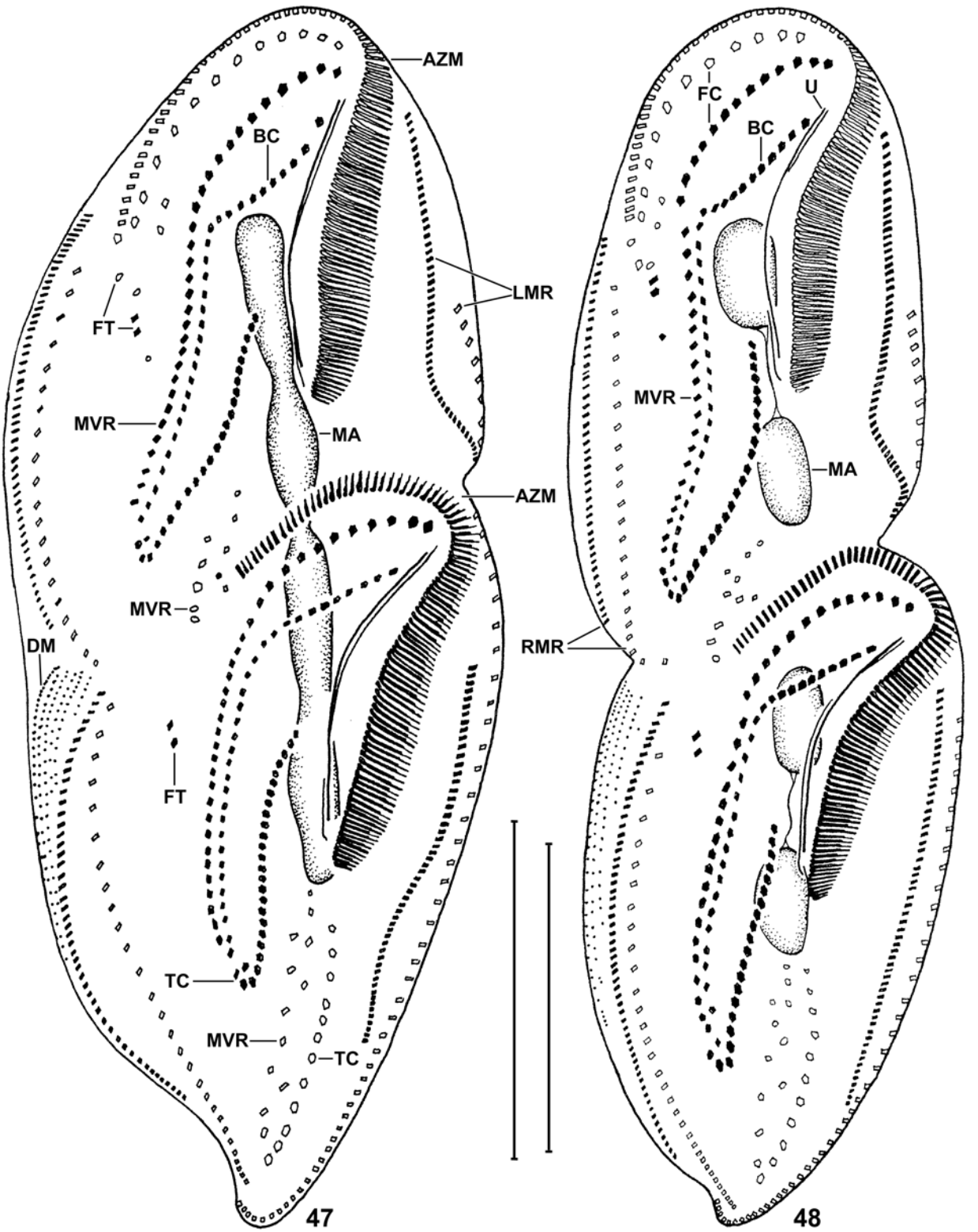

Figs 47, **48.** *Neokeronopsis* (*Afrokeronopsis*) *aurea*, ventral views of a late (47) and a very late (48) divider after protargol impregnation, showing, *inter alia*, the origin of the frontal (FC) and buccal (BC) cirral row from midventral cirral pairs. AZM – adoral zone of membranelles, BC – buccal cirral row, DM – dorsomarginal kineties, FC – frontal cirral coronas, FT – frontoterminal cirri, LMR – left marginal rows, MA – macronucleus nodules, MVR – midventral rows, RMR – right marginal rows, TC – transverse cirral rows, U – undulating membranes. Scale bars: 100 μm.

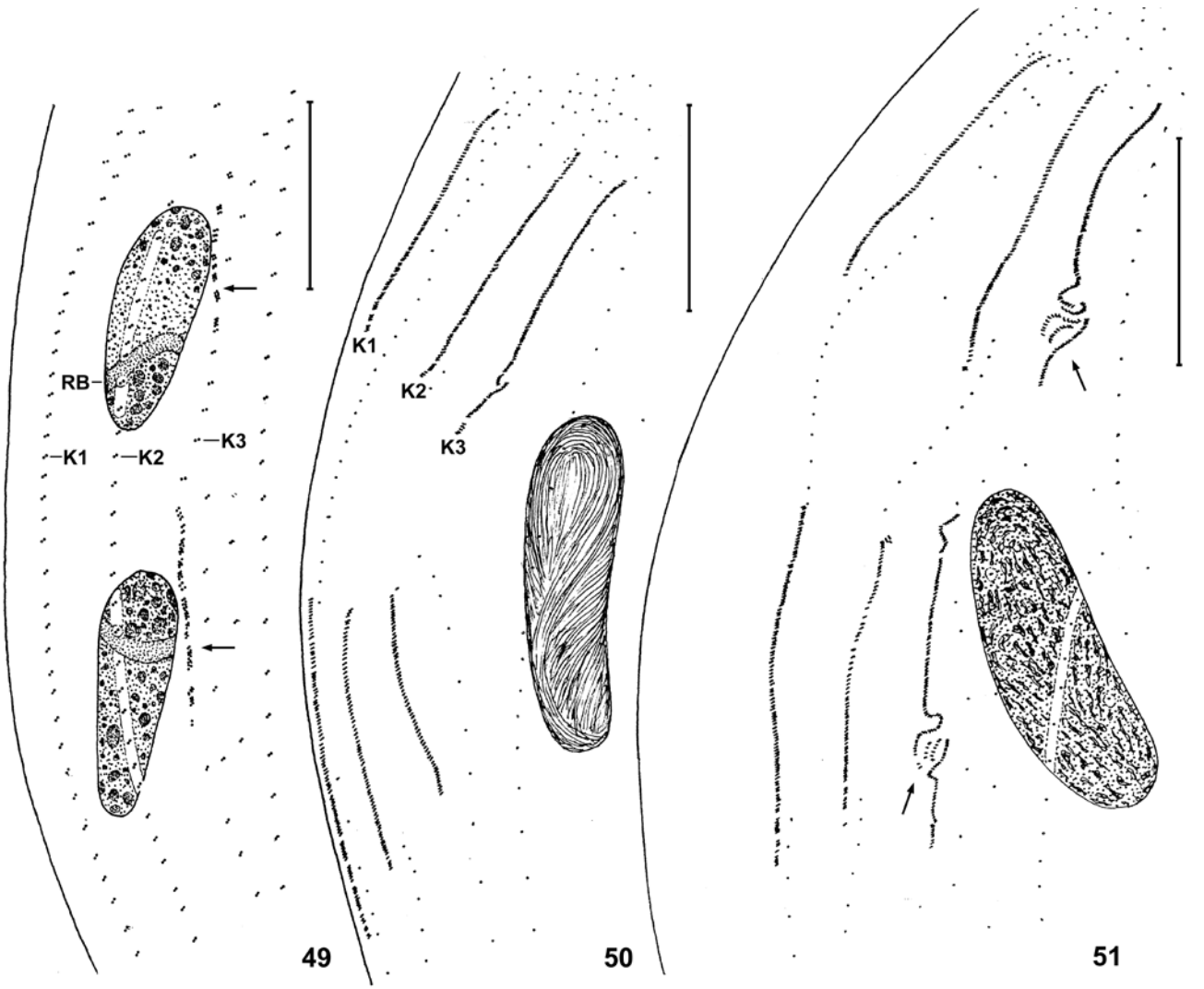

Figs 49–51. *Neokeronopsis* (*Afrokeronopsis*) *aurea*, ontogenesis of macronucleus and dorsal ciliary pattern after protargol impregnation. Note that, beginning with Figure 50, the parental dorsal bristles are shown by single dots although still composed of dikinetids; further, some might lack because they did not impregnate. **49** – very early divider showing the macronuclear reorganization band and the begin of dorsal ontogenesis (anlagen formation) within kinety 3 (arrows); **50** – early divider showing many curved fibres in the macronucleus nodules (only one is depicted). Dikinetidal anlagen have developed in kineties 1–3; **51** – early mid-divider showing many granules in the fibrous ground mass of the macronucleus nodules (only one is shown). A conspicuous whirl develops near to the posterior end of kinety 3 (arrows). K1–K3 – dorsal kineties, RB – reorganization band. Scale bars: 50 µm.

relative of the semiflexible *N.* (*A.*) *aurea* in all phylogenetic analyses. We here only show the evolutionary distance and Bayesian phylogeny (Fig. 38). The MP and the ML trees as well as trees from the calculations mentioned in the method section are available from the authors upon request. Note the often low bootstrap values, showing that the trees are far from being settled.

Reinvestigation of *N.* (*N.*) *spectabilis*

Warren *et al*. (2002) based the redescription of *N.* (*N.*) *spectabilis* on specimens prepared with Wilbert's protargol method. The cells are distributed over four slides, each possibly representing a separate preparation. We re-analysed the slides for several features possibly differing in *N.* (*N.*) *spectabilis* and *N.* (*A.*) *aurea*.

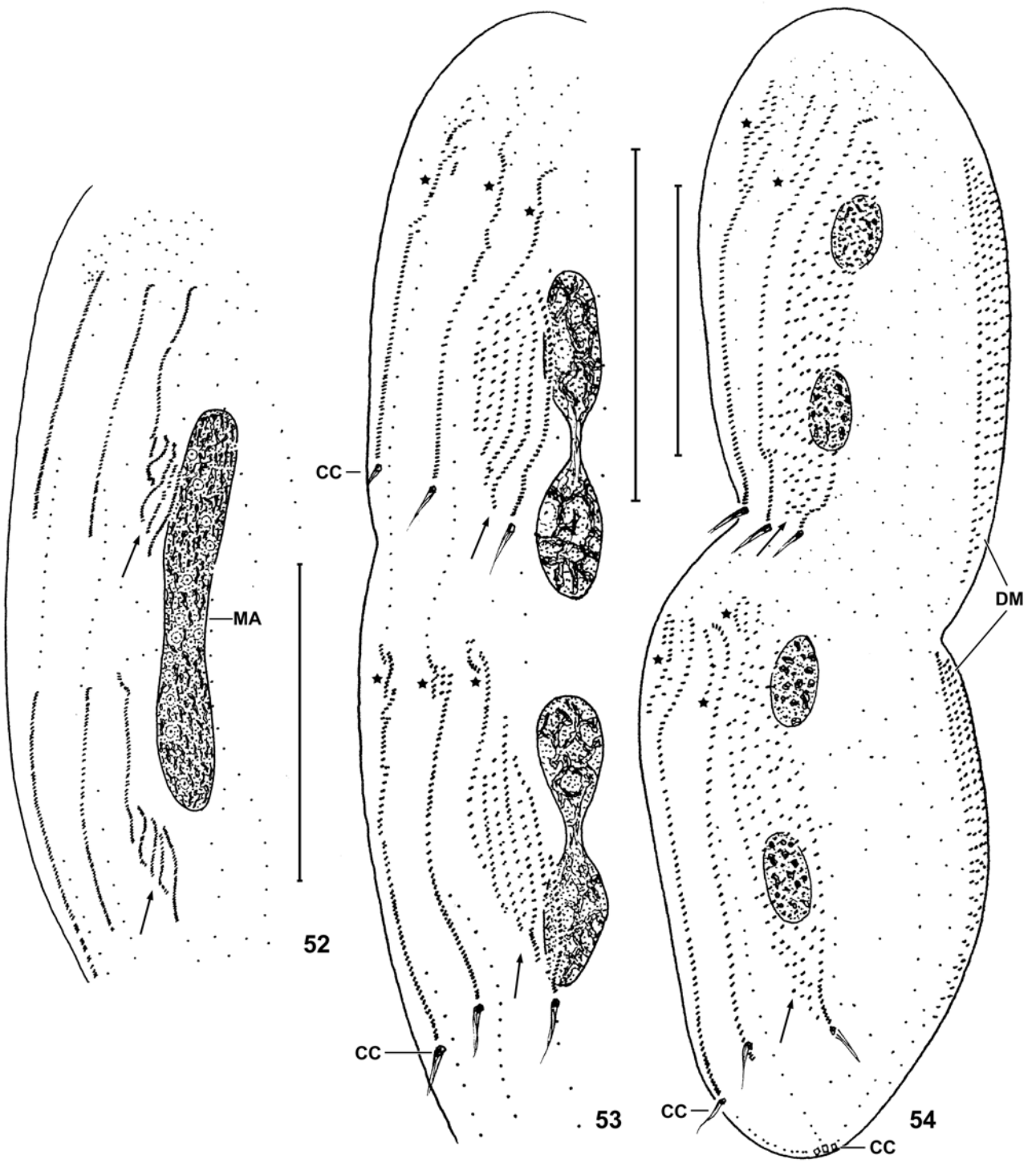

Figs 52–54. *Neokeronopsis* (*Afrokeronopsis*) *aurea*, ontogenesis of macronucleus and dorsal ciliary pattern after protargol impregnation. The parental dorsal bristles, some of which might be lacking due to insufficient impregnation, are shown by single dots although still composed of dikinetids. **52** – late mid-divider with elongating macronuclear mass showing numerous small aggregations in the finely granular ground mass. Arrows denote posterior multiple fragmentation of kinety 3; **53**, **54** – late (53) and very late (54) dividers finishing macronucleus division. Arrows mark growing kinetofragments of kinety 3. Asterisks denote anterior fragmentation of kineties 1–3, a unique and thus most important feature of the new subgenus *Afrokeronopsis*. Note dorsomarginal kineties along right body margin (cp. Figs 44, 46, 48) and developing caudal cirri at posterior end of kineties 1–3. CC – caudal cirri, DM – dorsomarginal kineties, MA – macronucleus. Scale bars: 100 μm.

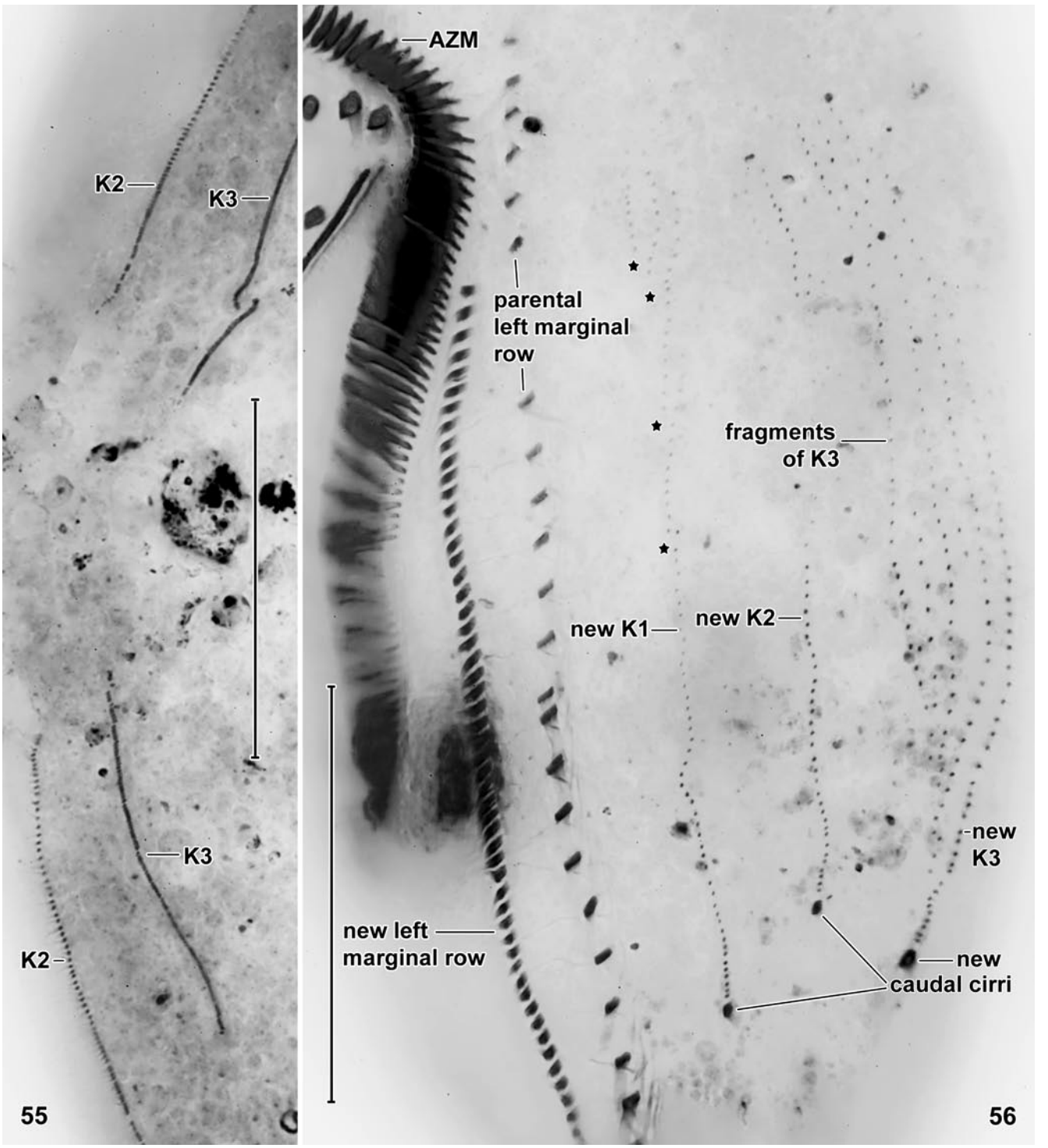

Figs 55, **56.** *Neokeronopsis* (*Afrokeronopsis*) *aurea*, dorsal ciliary pattern of dividers after protargol impregnation. **55** – early divider showing anlagen development in dorsal kineties 2 and 3 (cp. Fig. 50); **56** – late divider showing multiple anterior fragmentation of kinety 1 (asterisks) and multiple fragmentation in posterior region of kinety 3. Due to these fragmentations and the many dorsomarginal kineties (Fig. 54), the large dorsal side becomes covered with cilia. Scale bars: 50 µm.

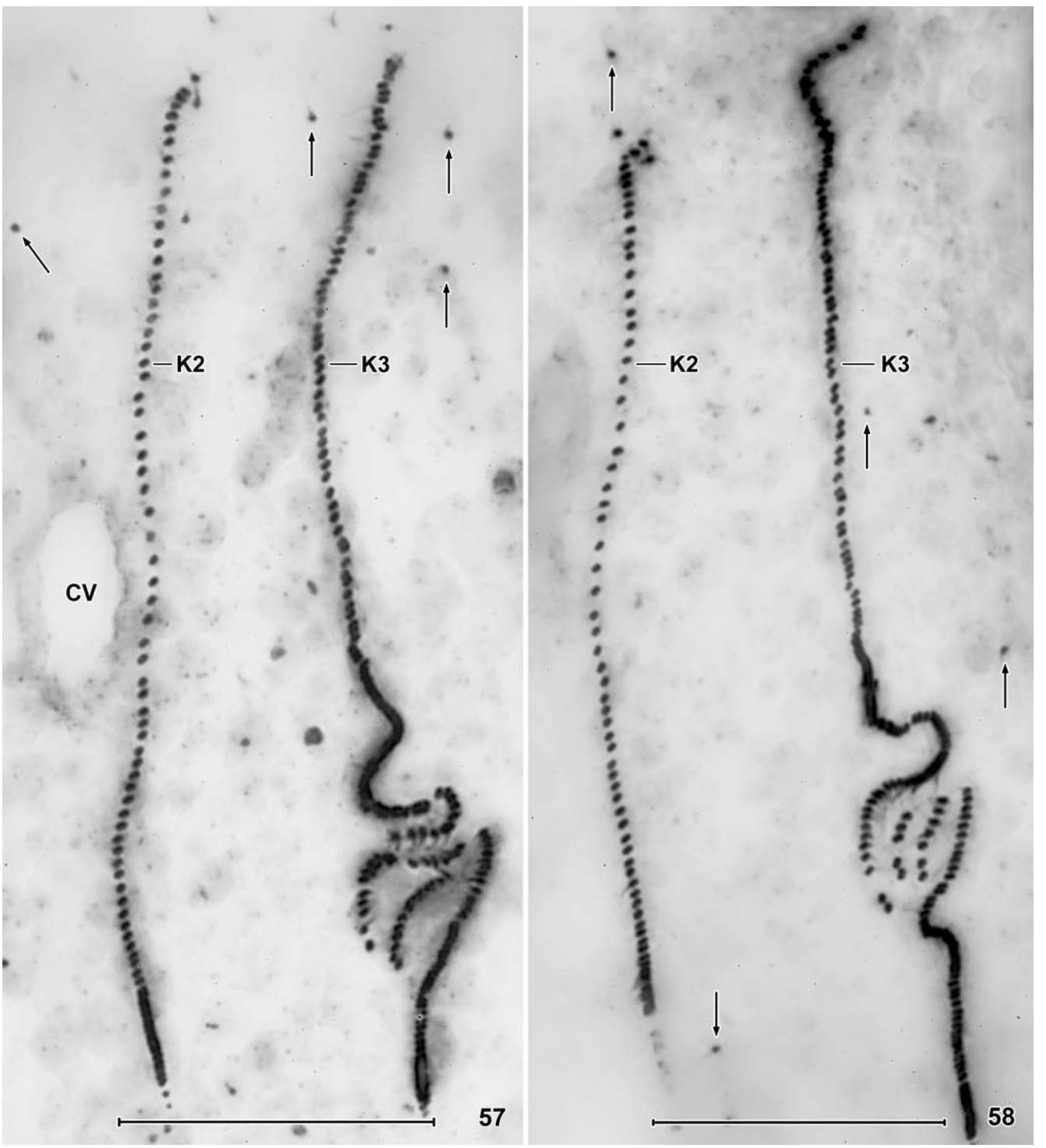

Figs 57, **58.** *Neokeronopsis* (*Afrokeronopsis*) *aurea*, proter and opisthe of an early mid-divider, showing the anlagen of dorsal kineties 2 and 3 (cp. Fig. 51). The anlagen consist of obliquely arranged, closely spaced dikinetids with short cilia. Kinety 3 commences multiple posterior fragmentation by forming a conspicuous whirl of kinetofragments. This is a unique mode of fragmentation and thus an important feature of the genus *Neokeronopsis*. Arrows mark some parental dorsal bristles still consisting of dikinetids. CV – opening of the contractile vacuole, K2, 3 – dorsal kineties. Scale bars: 20 μm.

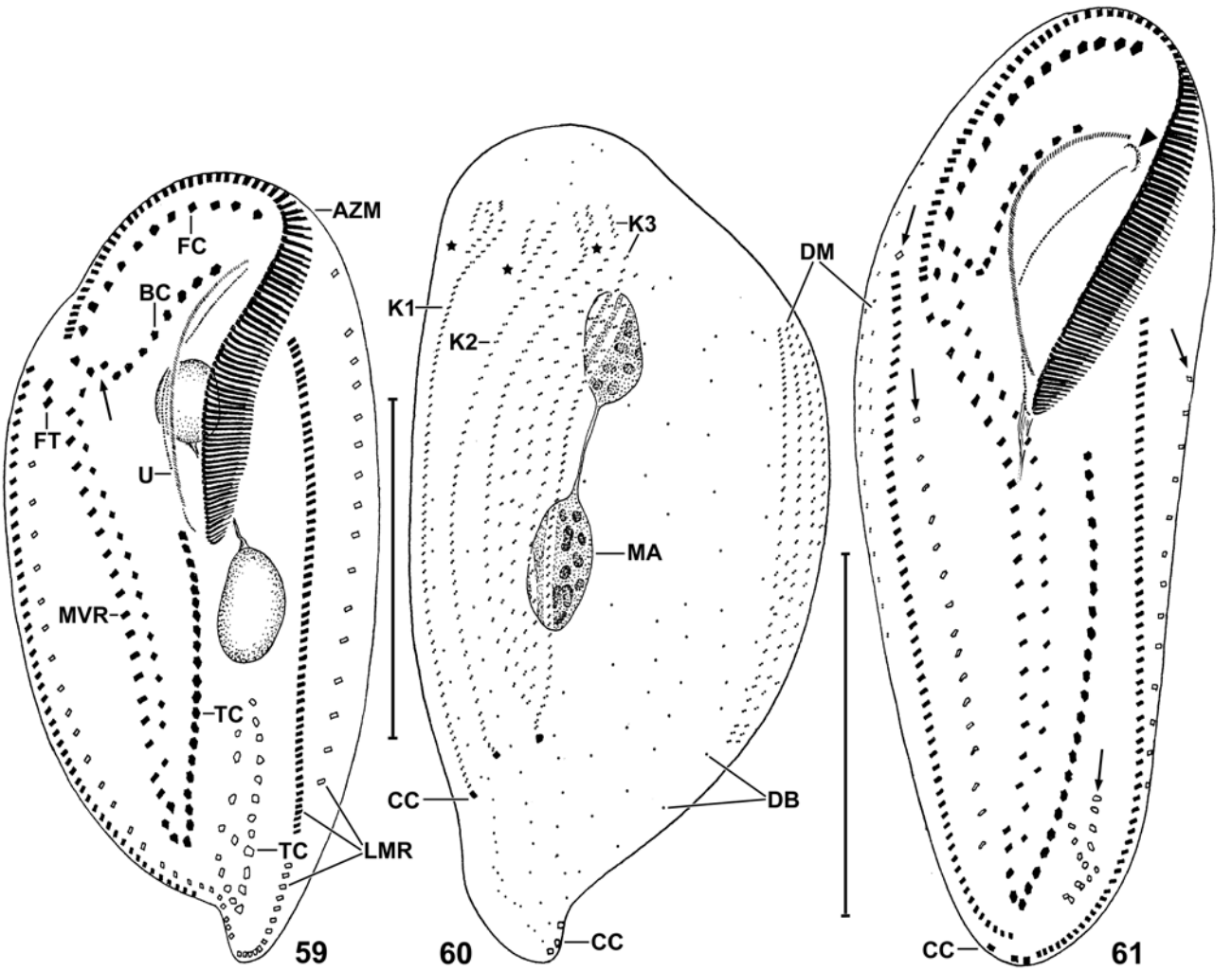

Figs 59–61. *Neokeronopsis* (*Afrokeronopsis*) *aurea*, post-dividers after protargol impregnation. **59**, **60** – ventral and dorsal view of early opisthe post-dividers. Still, much of the parental cirral pattern is recognizable, especially the marginal rows. The arrow marks the transition zone of the left row of midventral cirri and the buccal cirral row, while the frontal corona (FC) is the anterior portion of the right row of midventral cirri. Asterisks denote anterior fragments of dorsal kineties 1–3; **61** – ventral view of a late opisthe post-divider. Body, buccal cavity, and adoral zone of membranelles obtained the species-specific shape and the cirri arranged in interphase pattern, though some parental cirri have not yet resorbed (arrows). The triangle marks the developing buccal depression. AZM – adoral zone of membranelles, BC – buccal cirral row, CC – caudal cirri, DB – parental dorsal bristles, DM – dorsomarginal kineties, FC – frontal cirral corona, FT – frontoterminal cirri, K1–3 – dorsal kineties, LMR – left marginal rows, MA – macronucleus nodules, MVR – midventral rows, TC – transverse cirral row, U – undulating membranes. Scale bars: 100 μm.

(i) The paroral membrane does not consist of dikinetids throughout, as stated by Warren *et al*. (2002), but forms short, oblique kineties in the curved region, quite similar as in *Pattersoniella vitiphila* Foissner, 1987 and in *Cyrtohymena* (*Cyrtohymenides*) *aspoecki* Foissner, 2004. In contrast, the paroral membrane of *N.* (*A.*) *aurea* consists of short kineties throughout (Figs 14, 27, 37).

(ii) There is no indication of a buccal depression in the Polish population of *N.* (*N.*) *spectabilis*, not even in underbleached, rather darkly impregnated cells with well preserved buccal cavity. Furthermore, the anterior end of the paroral and endoral are very near together in most specimens, hardly leaving space for a buccal depression similar to that found in *N.* (*A.*) *aurea* (Figs 1, 9, 14, 25, 27).

(iii) Except of a single specimen, which looks like that figured in Warren *et al*. (2002), all well impregnated cells show multiple fragmentation of dorsal kinety 1,

especially in the posterior half (anterior half in *N.* (*A.*) *aurea*), while only one long or no fragment is present in the anterior half; further, kineties 2 and 3 possibly do not fragment anteriorly. The figures of the Chinese population of *N.* (*N.*) *spectabilis* indicate lack of any fragmentation (Wang *et al*. 2007). Thus, the fragmentation pattern of dorsal kineties 1–3 is distinctly different in the Polish and Chinese populations of *N.* (*N.*) *spectabilis*, and in *N.* (*A.*) *aurea*.

(iv) The few dividers contained in the slides are not in a stage to show whirl formation in dorsal kinety 3 (Figs 51, 57, 58).

DISCUSSION

The origin of the buccal cirri

There are one or several "buccal cirri" at the right margin of the buccal cavity (for a discussion of terminological matters, see Berger 1999). Usually, these cirri originate from cirral anlage II, even in genera which have, like *Neokeronopsis*, a bicorona, for instance, *Pseudokeronopsis* (Berger 1999, 2006; Fig. 65). Depending on the size of the anlage, one or several buccal cirri are generated. Rarely, the buccal cirrus has been lost, e.g., in *Paragastrostyla*, or has been incorporated in the frontal bicorona, as in *Uroleptopsis* (Berger 2006).

Neokeronopsis and *Pattersoniella* are the great, as yet unrecognized exceptions: they generate the anteriormost buccal cirrus in the ordinary way, i.e., from cirral anlage II, while the following are midventral cirri, i.e., originate from the anterior portion of the left midventral row (Figs 62–64). At first glance, these cirri are hardly recognizable as buccal cirri because the row extends obliquely away from the margin of the buccal cavity (Figs 62, 63). Indeed, Berger (2006) defines *Neokeronopsis* as having a bicorona ("two arched rows of frontal cirri"), obviously not recognizing the buccal nature of the inner cirral arch. The same applies to Wang *et al*. (2007). However, the ontogenetic data show that the inner cirral bow is composed of buccal cirri, both in *N.* (*N.*) *spectabilis* (Wang *et al*. 2007) and *N.* (*A.*) *aurea*, where the various transition stages are especially distinct (Figs 46–48, 59, 61).

We consider these two modes of buccal cirri production as a rather fundamental difference, showing not only the close relationship of *Pattersoniella* and *Neokeronopsis*, but also their distinctness within the hypotrichs, providing further reason for the family classification suggested in the present study and by Foissner and Stoeck (2006).

Structures of different origin should be separated terminologically. Thus, we suggest the term "pseudobuccal cirri" for cirri located like buccal cirri but not originating form cirral anlage II. This distinction does not exclude to use "buccal cirri" as a general term for both, e.g., when their origin is not important in the context used. The pseudobuccal cirri are not identical with the malar and paramalar cirri coined by Borror (for a discussion of these terms, see Berger 1999, 2006).

Body flexibility, cortical granules, and cirral pattern: the demise of time-honoured phylogenetic markers

Neokeronopsis is the fourth oxytrichid clade with midventral cirral rows (Foissner *et al*. 2004, Foissner and Stoeck 2006), suggesting the cirral pattern as an ambiguous phylogenetic marker. This is sustained by a recent molecular study (Schmidt *et al*. 2007), which indicates that even the "conservative" (Berger 1999, 2006) 18 frontal-ventral-transverse oxytrichid cirral pattern evolved convergently several times. Further, *N.* (*A.*) *aurea* has cortical granules, although it is (semi)rigid, a feature as yet found only in the flexible species of the Oxytrichinae (Berger 1999, Foissner *et al*. 2004). Obviously, *N.* (*A.*) *aurea* breaks both, the flexibility – and the granule dogma (Foissner *et al*. 2004, Foissner and Stoeck 2006). All these features evolved several (perhaps many) times in different lineages of the hypotrichs. Thus, they cannot be used longer as reliable phylogenetic markers, leaving various ontogenetic features, such as the origin of the ventral and dorsal ciliary pattern and the behaviour of the nuclear apparatus (nodules divide individually or fuse to divide as a single mass). But can we trust in the ontogenetic markers? The present state of knowledge suggests, we can although their interpretation is not easy. For instance, is the special mode of forming the buccal cirri in *Neokeronopsis* and *Pattersoniella* a reliable ontogenetic marker for a close relationship or evolved it convergently?

The widespread occurrence of convergences might be one of several reasons for the poor match of classic and molecular phylogenies in hypotrichs (Foissner *et al*. 2004, Schmidt *et al*. 2007). However, we emphasize that the molecular phylogenies are also controversial, possibly because they are based on a single gene (18S rDNA), of which we know that it is often too conservative for the classification of families and genera. All these problems show the urgent need of a combined clas-

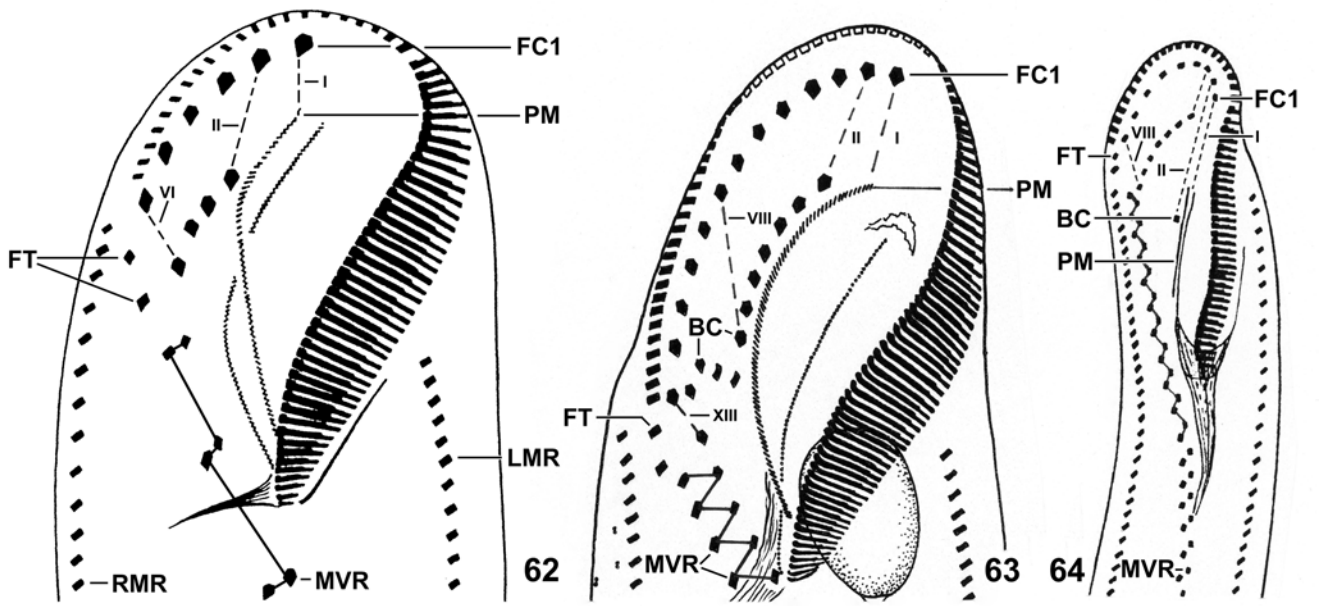

Figs 62–64. The two modes of origin of buccal cirri in hypotrichs (figures from Foissner 1987 and Berger 2006; modified). Cirri originating from the same anlage (marked by Roman numerals) are connected by hatched lines, while the cirri of the midventral rows are connected by solid lines. *Pseudokeronopsis* (64) and most other hypotrichs produce one or several buccal cirri from cirral anlage II, while the buccal cirri of *Pattersoniella vitiphila* (62) and *Neokeronopsis* (*N.*) *spectabilis* originate from many anlagen, which becomes evident when they are compared with the transition stages found in *Neokeronopsis* (*Afrokeronopsis*) *aurea* (Figs 46, 48, 59, 61, 63). Accordingly, *Pseudokeronopsis* has a "true" frontal bicorona, while *Pattersoniella* and *Neokeronopsis* have the inner arch composed of buccal cirri. Anlage I originates from the undulating membranes and invariably produces the first frontal cirrus. BC – buccal cirri, FC1 – frontal cirrus 1, FT – frontoterminal cirri, LMR – left marginal row, MVR – midventral rows, PM – paroral membrane, RMR – right marginal row, I, II, VIII, XIII – cirral anlagen.

sical and molecular approach, specifically, for detailed comparative ontogenetic and multigene analyses.

Neokeronopsis confirms the CEUU hypothesis

There are two highly characteristic cirral arrangements within the hypotrichs, viz., the oxytrichid and the urostylid pattern (Berger 1999, 2006; Foissner *et al*. 2004). The oxytrichid pattern typically consists of 18 cirri, i.e., 3 frontal, 5 frontoventral, 3 postoral, 2 pretransverse, and 5 transverse cirri (Fig. 38d). The urostylid pattern is characterized by two longitudinally extending rows with cirri arranged in a zigzagging "midventral pattern" (Figs 38a–c). Traditionally, these patterns are assigned to different families, viz., the Oxytrichidae and the Urostylidae (Borror 1972; Berger 1999, 2006; Foissner *et al*. 2004).

This classification was only partially supported by the molecular studies which showed that species with typical midventral pattern, i.e., *Uroleptus* spp. cluster within the 18 cirri Oxytrichidae (Hewitt *et al*. 2003, Foissner *et al*. 2004; Fig. 38). Foissner *et al*. (2004) tried to solve this dilemma by proposing the CEUU hypothesis (**C**onvergent **E**volution of midventral cirral rows in **U**rostylids and **U**roleptids) which suggests that the urostylid midventral pattern evolved from an oxytrichid ancestor and developed a second time from a different ancestor within the Oxytrichidae. Unfortunately, Foissner *et al*. (2004) could not provide a definite morphologic, ontogenetic, or molecular proof for the CEUU hypothesis. Such proof would have required a ciliate with the following combination of key features: midventral cirral pattern; fragmentizing dorsal kineties, preferably kinety 3; dorsomarginal kineties; and an oxytrichid 18S rDNA sequence. Obviously, *N.* (*A.*) *aurea* has all these attributes, and thus confirms the CEUU hypothesis. Likely, *N.* (*N.*) *spectabilis* will join as soon as its gene sequence is available.

Our gene tree (Fig. 38) suggests that a midventral cirral pattern evolved within the oxytrichids not only two times, as proposed by Foissner *et al*. (2004), but several times, viz., in *Pattersoniella*, *Uroleptus*, *Rigidothrix*, and *Neokeronopsis*. Likely, further such genera

await discovery and/or are misplaced at the present state of knowledge, for instance, *Territricha*, *Bicoronella*, *Afrophrya*, and *Holosticha stueberi* (for a detailed discussion of these taxa, see Foissner and Stoeck 2006).

CEUU hypothesis and molecular trees: consequences for the classification of hypotrichs and establishment of the new families Neokeronopsidae and Uroleptidae

The present and former investigations (Foissner *et al*. 2004, Foissner and Stoeck 2006) show an impressive fact (Fig. 38): an urostylid (midventral) cirral pattern evolved at least four times within the flexible oxytrichids, viz., in *Uroleptus*, *Pattersoniella*, *Rigidothrix* and *Neokeronopsis*. When Foissner *et al*. (2004) proposed the CEUU hypothesis, the sequences of *Rigidothrix* and *Neokeronopsis* were not yet known. Thus, Foissner *et al*. (2004) did not comment on classification of *Uroleptus*. Now, however, time is ripe for conclusions from the CEUU hypothesis and the sequence data accumulated. Each of the "midventral oxytrichids" is associated with a distinct molecular position, showing that they evolved independently in different evolutionary lines of the oxytrichids: *Pattersoniella* appears in the rigid clade, *Rigidothrix* clusters near *Oxytricha*, *Neokeronopsis* clusters with the *Paraurostyla-Cyrtohymena* group, and *Uroleptus* forms its own cluster between the two others (Fig. 38). In accordance with Foissner and Stoeck (2006), we thus propose a distinct family for each of the "midventral oxytrichids." Although this is not supported by monophylies in the molecular trees, possibly due to insufficient taxon sampling and a low resolution of the hypotrich SSU rDNA in general (Foissner *et al*. 2004, Schmidt *et al*. 2007), it is warranted by the morphologic and ontogenetic data (for reviews, see Berger 1999, 2006), i.e., hypotrichs with oxytrichid, respectively, urostylid cirral pattern should not remain in the same family because they represent highly distinct evolutionary lines. Ranking this difference only at genus level would create a massive disproportionality to many other genera often separated only by the presence *vs.* absence of transverse cirri or by the pattern formed by the undulating membranes. Figure 65 presents a Hennigian argumentation scheme which summarizes the present and former hypotheses.

Family Neokeronopsidae: for definition, see Result section. Here we provide the theoretical background (above) and some important details.

Kahl (1932), who discovered *N.* (*N.*) *spectabilis*, classified it close to *Holosticha* due to the midventral cirral pattern. Today, hypotrichs with midventral pattern are usually assigned to the Urostyloidea (Berger 2006). Based on a detailed redescription and some ontogenetic data, Warren *et al*. (2002) recognized that *N.* (*N.*) *spectabilis* has features from both, the oxytrichids (e.g., fragmentation of dorsal kinety 3) and the urostylids (e.g., midventral cirral pattern). Thus, they concluded that placement of *Neokeronopsis* within the Urostylidae remains uncertain. Berger (2006), in contrast, classified *Neokeronopsis* in the Oxytrichidae, but emphasized the need of molecular data. Very recently, Wang *et al*. (2007) provided more complete ontogenetic data and concluded that *N.* (*N.*) *spectabilis*, "very likely represents an intermediate form between oxytrichids and urostylids". The ontogenetic and molecular data from *N.* (*A.*) *aurea* support the classifications of Berger (2006) and Foissner and Stoeck (2006), who considered *Neokeronopsis* a derived oxytrichid with a secondarily evolved midventral cirral pattern, quite similar to *Uroleptus* spp. (Foissner *et al*. 2004) and *Rigidothrix goiseri* (Foissner and Stoeck 2006). This is in accordance with the CEUU hypothesis which suggests that a midventral pattern evolved at least two times: the first, older event caused the ancestor to split into an oxytrichid and an urostylid lineage, while the second, more recent event caused the development of a midventral pattern in several oxytrichid lineages (Fig. 64).

The molecular analyses indicate a close relationship of *Neokeronopsis* with *Cyrtohymena*, as suggested by Berger (2006), based on the presence of cortical granules and the cyrtohymenid oral apparatus (Fig. 38). However, the *Paraurostyla – Cyrtohymena – Neokeronopsis* cluster has low bootstrap support (59/< 50/< 50), indicating that it could merge with the large cluster containing *Pattersoniella*, if taxon sampling is increased. Indeed *N.* (*A.*) *aurea* has two highly specific traits in common with *Pattersoniella*, viz., the production of buccal cirri from the midventral rows (Figs 46–48) and the buccal depression (Fig. 9) found also in *Steinia*, a close molecular relative of *Pattersoniella* (Fig. 38). Thus, we disagree with Berger (2006) who excluded a close relationship of *Pattersoniella* and *Neokeronopsis*.

Certainly, the molecular trees indicate that even special and thus "strong" characteristics, such as the buccal depression and the uncommon mode of forming the buccal cirri, could have evolved convergently. On the other hand, the poor bootstrap support of the *Neokeronopsis* clade (Fig. 38) and the low resolution of the hypotrich SSU rDNA in general (Foissner *et al*. 2004, Schmidt *et al*. 2007) warrant to interpret the molecu-

lar trees as critically as the morphologic ones. At the present state of knowledge, the inclusion of *Pattersoniella* in the Neokeronopsidae avoids the creation of a further family, as explained in the first paragraph of this chapter.

Family Uroleptidae: for definition, see Result section. Here, we provide the justification (first paragraph of chapter) and some important notes.

The diagnosis is based on the molecular data (Fig. 38). However, if it is assumed that *Rigidothrix* lost dorsal kinety fragmentation (Fig. 65), then the uroleptids can be clearly defined also morphologically: very flexible midventral oxytrichids lacking fragmentizing dorsal kineties.

Uroleptus, type genus of the family, is full of problems which should be solved by a detailed revision of the group. However, Kahl (1932), Foissner *et al*. (1991), and Berger (2006) addressed some issues, especially, they confined *Uroleptus* to species with midventral cirral pattern. Another major problem concerns the distinction from *Holosticha* and several other urostylids because *Uroleptus* differs from these genera only by the slender, more or less pisciform body shape (Kahl 1932, Foissner *et al*. 1991). However, the molecular data show that *Uroleptus*, indeed, is very different from the holostichids: the former belongs to the oxytrichids, the latter to the urostylids (Foissner *et al*. 2004, Berger 2006, Schmidt *et al*. 2007). Based on this knowledge, Berger (2006) established an unranked taxon, the Dorsomarginalia, which include all ordinary and midventral oxytrichids. We agree, but suggest family rank for the Oxytrichinae and Stylonychinae (Fig. 65).

Generic classification of *Neokeronopsis* (*Afrokeronopsis*) aurea

Neokeronopsis (*Neokeronopsis*) *spectabilis* and *Neokeronopsis* (*Afrokeronopsis*) *aurea* differ by several distinct features possibly useful for generic or subgeneric separation. Unfortunately, the descriptions of *N.* (*N.*) *spectabilis* are not as detailed as one would wish, and the reinvestigation of the preparations from the Polish population could not eliminate all uncertainties (see Result section). Further, gene sequences are available only from *N.* (*A.*) *aurea*. Accordingly, we separate the African species only at subgeneric level from the Eurasian counterpart, emphasizing both similarities and differences.

The buccal depression is a highly characteristic feature of *N.* (*A.*) *aurea* (Figs 25, 27–29). So far, a buccal depression was known only from the genus *Steinia* (Kahl 1932, Foissner 1989, Berger 1999), i.e., has not been mentioned in the four descriptions of *N.* (*N.*) *spectabilis* (Kahl 1932, Warren *et al*. 2002, Berger 2006, Wang *et al*. 2007). The reinvestigation of the Polish population indicates that a buccal depression is, indeed, absent from *N.* (*N.*) *spectabilis*. However, live observation is required to be entirely sure. Certainly, this feature is a "strong" generic character.

The paroral membrane is composed of short, oblique kineties in *N.* (*A.*) *aurea* (Figs 16, 27, 37) and of a double row of basal bodies (dikinetids) in *N.* (*N.*) *spectabilis* (Warren *et al*. 2002). However, the reinvestigation of the Polish *N.* (*N.*) *spectabilis* showed the presence of short, oblique kineties in, at least, the curved portion of the paroral membrane. Thus, this feature is useful only at species level.

Neokeronopsis (*Afrokeronopsis*) *aurea* has 3 caudal cirri (Table 1), while *N.* (*N.*) *spectabilis* has an average of about 9 (Warren *et al*. 2002, Wang *et al*. 2007). Usually, the number of caudal cirri is not used as a generic feature. However, this might be too conservative because most hypotrichs have 3 caudal cirri, and thus a considerably increased number might indicate a distinct evolutionary branch.

Neokeronopsis (*Neokeronopsis*) *spectabilis* develops the oral primordium from three anlagen, i.e., from two small fields underneath the buccal vertex and a narrow field anterior and along the upper three transverse cirri (Wang *et al*. 2007). In contrast, *N.* (*A.*) *aurea* generates the oral primordium along the upper 8–11 cirri of the transverse cirral row (Fig. 17); this has been checked in three specimens. Usually, such difference is not used as a generic character, but in combination with other features it appears a useful discriminator.

The anterior fragmentation of dorsal kineties 1–3 in *N.* (*A.*) *aurea* is an outstanding feature as yet not observed in any other hypotrich (Figs 15, 20, 26). Likely, the fragmentation serves to fill the large anterior area with dorsal (sensory?) bristles. Warren *et al*. (2002) and Wang *et al*. (2007) do not mention such fragmentation in *N.* (*N.*) *spectabilis*. However, Figure 18 in Warren *et al*. (2002) and Figure 30 in Wang *et al*. (2007) indicate some fragmentation of kineties 1 and 2; on the other hand, Figure 15 in Wang *et al*. (2007) excludes this possibility. Our reinvestigation shows that Warren *et al*. (2002) overlooked fragmentation in *N.* (*N.*) *spectabilis*. However, details are markedly different, suggesting that this feature is useable for, at least, species distinction. The micrographs in Wang *et al*. (2007) show a long

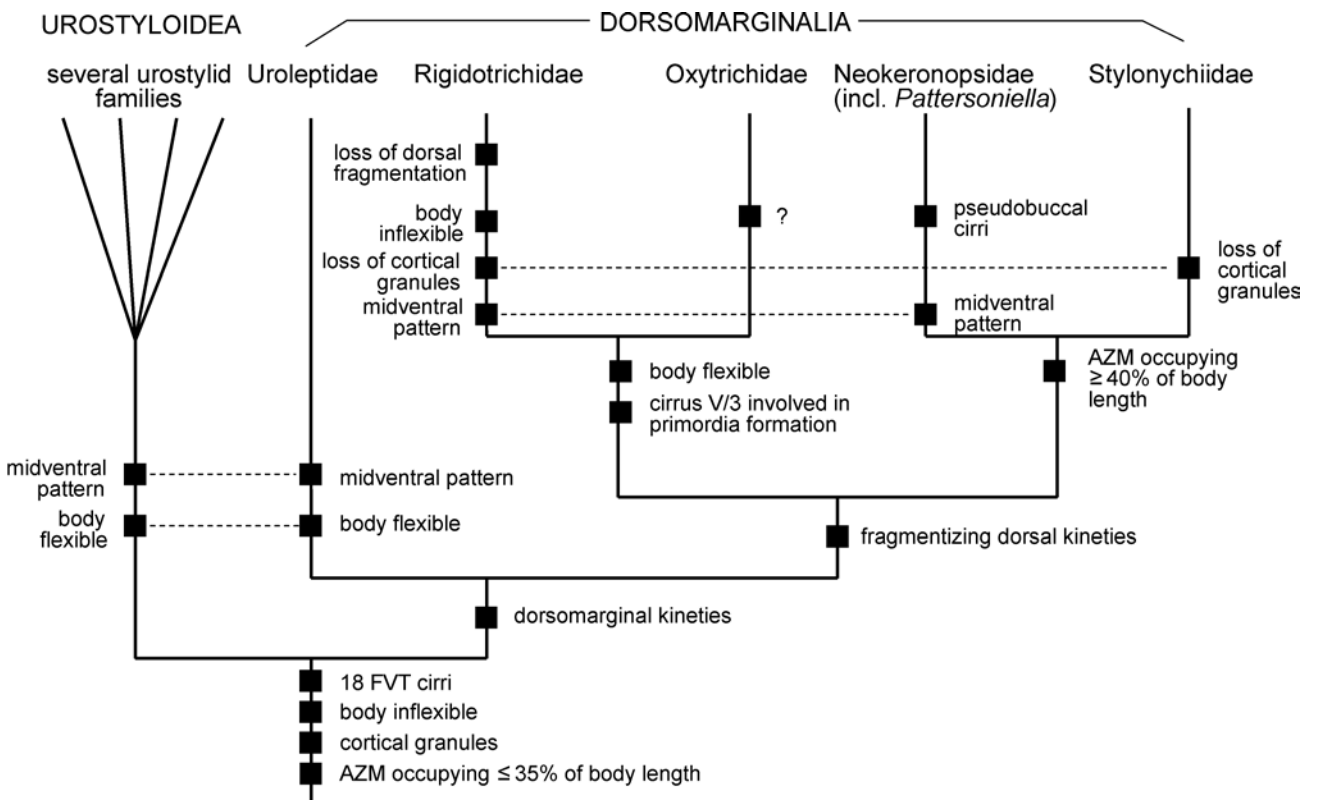

Fig. 65. A cladistic (Hennigian) argumentation scheme for some main hypotrich lineages, based on the morphologic and ontogenetic data reported by Foissner *et al*. (2004), Foissner and Stoeck (2006), Berger (1999, 2006), and the present paper. See these studies for a detailed explanation of characters and character states. Hatched lines indicate convergences. As concerns classification within the Urostyloidea, see Berger (2006).

anterior fragment near dorsal kinety 1, while multiple posterior fragmentation, which is so prominent in the Polish specimens, is apparently absent. Thus, the Chinese population possibly represents a distinct species. To be sure, very late dividers and post-dividers should be restudied.

Neokeronopsis (*Afrokeronopsis*) *aurea* as a new species

We did not find any species in the literature that could be identical with *N.* (*A.*) *aurea*. It differs from *N.* (*N.*) *spectabilis*, as described by Kahl (1932) and redescribed by Warren *et al*. (2002), Berger (2006) and Wang *et al*. (2007), not only by the subgeneric features outlined in the previous section but also by the following details: (i) although body size is similar or larger in *N.* (*N.*) *spectabilis*, the number of cirri and adoral membranelles is on average higher by 15–30% in *N.* (*A.*) *aurea*; (ii) the cortical granulation is distinct not only dorsally but also ventrally, especially left of the cirri of the frontal corona (Figs 3–5, 28); (iii) the macronucleus nodules are connected by a fine strand (Fig. 15); (iv) the transverse cirral row extends much farther anteriorly in *N.* (*A.*) *aurea* than in *N.* (*N.*) *spectabilis* due to both a slightly higher number and wider spacing of the cirri (Figs 1, 14, 18); (v) the right end of the adoral zone of membranelles extends much farther posteriorly in *N.* (*A.*) *aurea* than in *N.* (*N.*) *spectabilis* (Figs 1, 19, 25); (vi) the buccal cirral row is distinctly closer to the margin of the buccal cavity in *N.* (*A.*) *aurea* than in *N.* (*N.*) *spectabilis* (Figs 1, 14, 25); (vii) the paroral membrane is less distinctly curved in *N.* (*A.*) *aurea* than in *N.* (*N.*) *spectabilis*, where it almost abuts to the anterior end of the endoral membrane (Figs 14, 18, 25).

Possibly, *N.* (*A.*) *aurea* represents the plesiomorphic state, i.e., is the ancestor of *N.* (*N.*) *spectabilis*. This is indicated by the oral primordium which develops along the anterior half of the transverse cirral row in *N.* (*A.*) *aurea*, while mainly above the transverse cirral row in

N. (*N.*) *spectabilis*. Obviously, the transverse cirral row has been shortened in *N.* (*N.*) *spectabilis*.

Biogeographic aspects

Both *N.* (*N.*) *spectabilis* and *N.* (*A.*) *aurea* are large, highly conspicuous species, representing ideal biogeographic flagships (Foissner 2006). Indeed, these two species provide an almost perfect proof for the restricted distribution of certain protist species because they occur in quite ordinary habitats (ponds, rivers and their floodplains) present all over the world. In spite of this, *N.* (*N.*) *spectabilis* has been recorded only from Eurasia, while *N.* (*A.*) *aurea* is possibly restricted to the Palaeotropis or Gondwana.

Neokeronopsis (*Afrokeronopsis*) *aurea* is, at present, known only from two floodplains in the Krueger National Park, Republic of South Africa, although we investigated several samples each from the Danube floodplain in Austria, the Amazon floodplain in Brazil, and the Murray River floodplain in Australia (Foissner 1997, 1998, 2007; Foissner *et al*. 2002; Chao *et al*. 2006). In contrast, eight Eurasian records, of which five are substantiated by detailed data, are known from *N.* (*N.*) *spectabilis* (Berger 2006): Austria, Germany, Slovakia, Poland, Ukraine, and China (Wang *et al*. 2007). If both, *N.* (*N.*) *spectabilis* and *N.* (*A.*) *aurea* were present in Eurasia, it would be highly unlikely that only *N.* (*N.*) *spectabilis* has been found; likewise, if both occur in the Krueger National Park, it would be unlikely that we found only one.

Acknowledgements. Financial support was provided by the Austrian Science Foundation (FWF project P-19699-B17) and the German Science Foundation (DFG, STO-414/2-3). The technical assistance of Mag. Birgit Weissenbacher, Mag. Gudrun Fuss, Robert Schörghofer, Hans-Werner Breiner and Andreas Zankl is greatly acknowledged. Special thanks to Dr. Alan Warren (British Museum of Natural History) for sending us slides from *N.* (*N.*) *spectabilis*.

REFERENCES

Augustin H., Foissner W. (1992) Morphologie und Ökologie einiger Ciliaten (Protozoa: Ciliophora) aus dem Belebtschlamm. *Arch. Protistenk.* **141:** 243–283

Berger H. (1999) Monograph of the Oxytrichidae (Ciliophora, Hypotrichia). *Monogr. Biol.* **78:** 1–1080

Berger H. (2006) Monograph of the Urostyloidea (Ciliophora, Hypotricha). *Monogr. Biol.* **85:** 1–1304

Berger H., Foissner W. (1989) Morphology and biometry of some soil hypotrichs (Protozoa, Ciliophora) from Europe and Japan. *Bull. Br. Mus. Nat. Hist.* (*Zool.*) **55:** 19–46

Borror A. C. (1972) Revision of the order Hypotrichida (Ciliophora, Protozoa). *J. Protozool.* **19:** 1–23

Bütschli O. (1889) Protozoa. III. Abteilung: Infusoria und System der Radiolaria. In: Klassen und Ordnungen des Thier-Reichs, wissenschaftlich dargestellt in Wort und Bild. (Ed. H. G. Bronn), Winter, Leipzig, pp. 1585–2035

Chao A., Li P. C., Agatha S., Foissner W. (2006) A statistical approach to estimate soil ciliate diversity and distribution based on data from five continents. *Oikos* **114:** 479–493

Corliss J. O. (1979) The Ciliated Protozoa. Characterization, Classification and Guide to the Literature. 2nd ed. Pergamon Press, Oxford, New York, Toronto, Sydney, Paris, Frankfurt

Ehrenberg C. G. (1830) Beiträge zur Kenntniß der Organisation der Infusorien und ihrer geographischen Verbreitung, besonders in Sibirien. *Abh. Preuss. Akad. Wiss., Phys. Math. Kl.* year 1830**:** 1–88

Ehrenberg C. G. (1831) Über die Entwickelung und Lebensdauer der Infusionsthiere; nebst ferneren Beiträgen zu einer Vergleichung ihrer organischen Systeme. *Abh. Preuss. Akad. Wiss., Phys.-math. Kl.* year 1831**:** 1–154

Ehrenberg C. G. (1838) Die Infusionsthierchen als vollkommene Organismen. Voss, Leipzig

Foissner W. (1987) Neue und wenig bekannte hypotriche und colpodide Ciliaten (Protozoa: Ciliophora) aus Böden und Moosen. *Zool. Beitr., N. F.* **31:** 187–282

Foissner W. (1989) Morphologie und Infraciliatur einiger neuer und wenig bekannter terrestrischer und limnischer Ciliaten (Protozoa, Ciliophora). *Sber. Akad. Wiss. Wien* **196:** 173–247

Foissner W. (1991) Basic light and scanning electron microscopic methods for taxonomic studies of ciliated protozoa. *Europ. J. Protistol.* **27:** 313–330

Foissner W. (1997) Soil ciliates (Protozoa: Ciliophora) from evergreen rain forests of Australia, South America and Costa Rica: diversity and description of new species. *Biol. Fertil. Soils* **25:** 317–339

Foissner W. (1998) An updated compilation of world soil ciliates (Protozoa, Ciliophora), with ecological notes, new records, and descriptions of new species. *Europ. J. Protistol.* **34:** 195–235

Foissner W. (2004) Some new ciliates (Protozoa, Ciliophora) from an Austrian floodplain soil, including a giant, red "flagship," *Cyrtohymena* (*Cyrtohymenides*) *aspoecki* nov. subgen., nov. spec. *Denisia* **13:** 369–382

Foissner W. (2006) Biogeography and dispersal of micro-organisms: a review emphasizing protists. *Acta Protozool*. **45:** 111–136

Foissner W. (2007) Dispersal and biogeography of protists: recent advances. *Jpn. J. Protozool.* **40:** 1–16

Foissner W., Adam H. (1983) Morphologie und Morphogenese des Bodenciliaten *Oxytricha granulifera* sp. n. (Ciliophora, Oxytrichidae). *Zool. Scr.* **12:** 1–11

Foissner W., Agatha S., Berger H. (2002) Soil ciliates (Protozoa, Ciliophora) from Namibia (Southwest Africa), with emphasis on two contrasting environments, the Etosha Region and the Namib Desert. *Denisia* **5:** 1–1459

Foissner W., Al-Rasheid K. (2006) A unified organization of the stichotrichine oral apparatus, including a description of the buccal seal (Ciliophora: Spirotrichea). *Acta Protozool.* **45:** 1–16

Foissner W., Blatterer H., Berger H., Kohmann F. (1991) Taxonomische und ökologische Revision der Ciliaten des Saprobiensystems – Band I: Cyrtophorida, Oligotrichida, Hypotrichia, Colpodea. *Informationsberichte Bayer. Landesamt für Wasserwirtschaft, München* **1/91:** 1–478

Foissner W., Moon-van der Staay S.Y., van der Staay G. W. M., Hackstein J. H. P., Krautgartner W.-D., Berger H. (2004) Recon-

ciling classical and molecular phylogenies in the stichotrichines (Ciliophora, Spirotrichea), including new sequences from some rare species. *Europ. J. Protistol.* **40:** 265–281

Foissner W., Stoeck, T. (2006) *Rigidothrix goiseri* nov. gen., nov. spec. (Rigidotrichidae nov. fam.), a new "flagship" ciliate from the Niger floodplain breaks the flexibility-dogma in the classification of stichotrichine spirotrichs (Ciliophora, Spirotrichea). *Europ. J. Protistol.* **42:** 249–267

Hewitt E. A., Müller K. M., Cannone J., Hogan D. J., Gutell R., Prescott D. M. (2003) Phylogenetic relationships among 28 spirotrichous ciliates documented by rDNA. *Molec. Phylogen. Evol.* **29:** 258–267

Kahl A. (1932) Urtiere oder Protozoa I: Wimpertiere oder Ciliata (Infusoria) 3. Spirotricha. *Tierwelt Dtl.* **25:** 399–650

Maddison D. R., Maddison W. P. (2003) McClade. Version 4.0. Sinauer Associates, Sunderland, MA

Medlin L., Elwood H. J., Stickel S., Sogin M. L. (1988) The characterization of enzymatically amplified eukaryotic l6S-like rRNA-coding regions. *Gene* **71:** 491–499

Petz W., Foissner W. (1996) Morphology and morphogenesis of *Lamtostyla edaphoni* Berger and Foissner and *Onychodromopsis flexilis* Stokes, two hypotrichs (Protozoa: Ciliophora) from Antarctic soils. *Acta Protozool.* **35:** 257–280

Posada D., Crandall K. A. (1998) MODELTEST: testing the model of DNA substitution. *Bioinformatics* **14:** 817–818

Ronquist F., Huelsenbeck J. P. (2003) MRBAYES 3: Bayesian phylogenetic inference under mixed models. *Bioinformatics* **19:** 1572–1574

Schmidt S. L., Bernhard D., Schlegel M., Foissner W. (2007) Phylogeny of the Stichotrichia (Ciliophora; Spirotrichea) reconstructed with nuclear small subunit rRNA gene sequences: discrepancies and accordances with morphological data. *J. Eukaryot. Microbiol.* **54:** 201–209

Shi X., Song W., Shi X. (1999) Systematic revision of the hypotrichous ciliates. In: Progress in Protozoology. (Ed. W. Song). Qingdao Ocean University Press, Qingdao, pp. 77–154

Stein F. (1859) Der Organismus der Infusionsthiere nach eigenen Forschungen in systematischer Reihenfolge bearbeitet. I. Abteilung. Allgemeiner Theil und Naturgeschichte der hypotrichen Infusionsthiere. W. Engelmann, Leipzig

Stoeck T., Epstein S. (2003) Novel eukaryotic lineages inferred from small-subunit rRNA analyses of oxygen-depleted marine environments. *Appl. Environ. Microbiol.* **69:** 2657–2663

Swofford D. L. (2002) PAUP* Phylogenetic analysis using parsimony (*and other methods). Version 4. Sinauer Associates, Sunderland, MA

Thompson J. D., Gibson T. J., Plewniak F., Jeanmougin F., Higgins D. G. (1997) The CLUSTAL–X windows interface: flexible strategies for multiple sequence alignment aided by quality analysis tools. *Nucleic. Acids Res.* **25:** 4876–4882

Tuffrau M. (1960) Révision du genre *Euplotes*, fondée sur la comparaison des structures superficielles. *Hydrobiologia* **15:** 1–77

Tuffrau M., Pyne C. K., Haller G. De (1968) Organisation de l'infraciliature chez quelques ciliés hypotriches. *Protistologica* **4:** 289–301

Voss H.-J., Foissner W. (1996) Divisional morphogenesis in *Steinia sphagnicola* (Ciliophora, Hypotrichida): a comparative light and scanning electron microscopic study. *Europ. J. Protistol.* **32:** 31–46

Wallengren H. (1900) Zur Kenntnis der vergleichenden Morphologie der hypotrichen Infusorien. *Bih. K. svensk VetenskAkad. Handl.* **26:** 1–31

Wang R., Qiu Z., Chen J., Warren A., Song W. (2007) Morphogenesis of the freshwater ciliate *Neokeronopsis spectabilis* (Kahl 1932) Warren *et al*., 2002, based on a China population (Ciliophora: Urostylidae). *J. Eukaryot. Microbiol.* **54:** 184–190

Warren A., Fyda J., Song W. (2002) The morphology of the poorly-known freshwater urostylid ciliate *Neokeronopsis spectabilis* (Kahl, 1932) nov. gen., nov. comb., (Ciliophora: Urostylidae), with notes on its morphogenesis. *Europ. J. Protistol.* **38:** 195–206

Received on 30th October, 2007; revised version on 3rd January, 2008; accepted on 3rd January, 2008